PHYSIOLOGICAL MEASUREMENTS OF THE HUMAN COUGHS AND SNEEZES

Sean Fitzgerald

Bachelor of Engineering
Mechanical Engineering
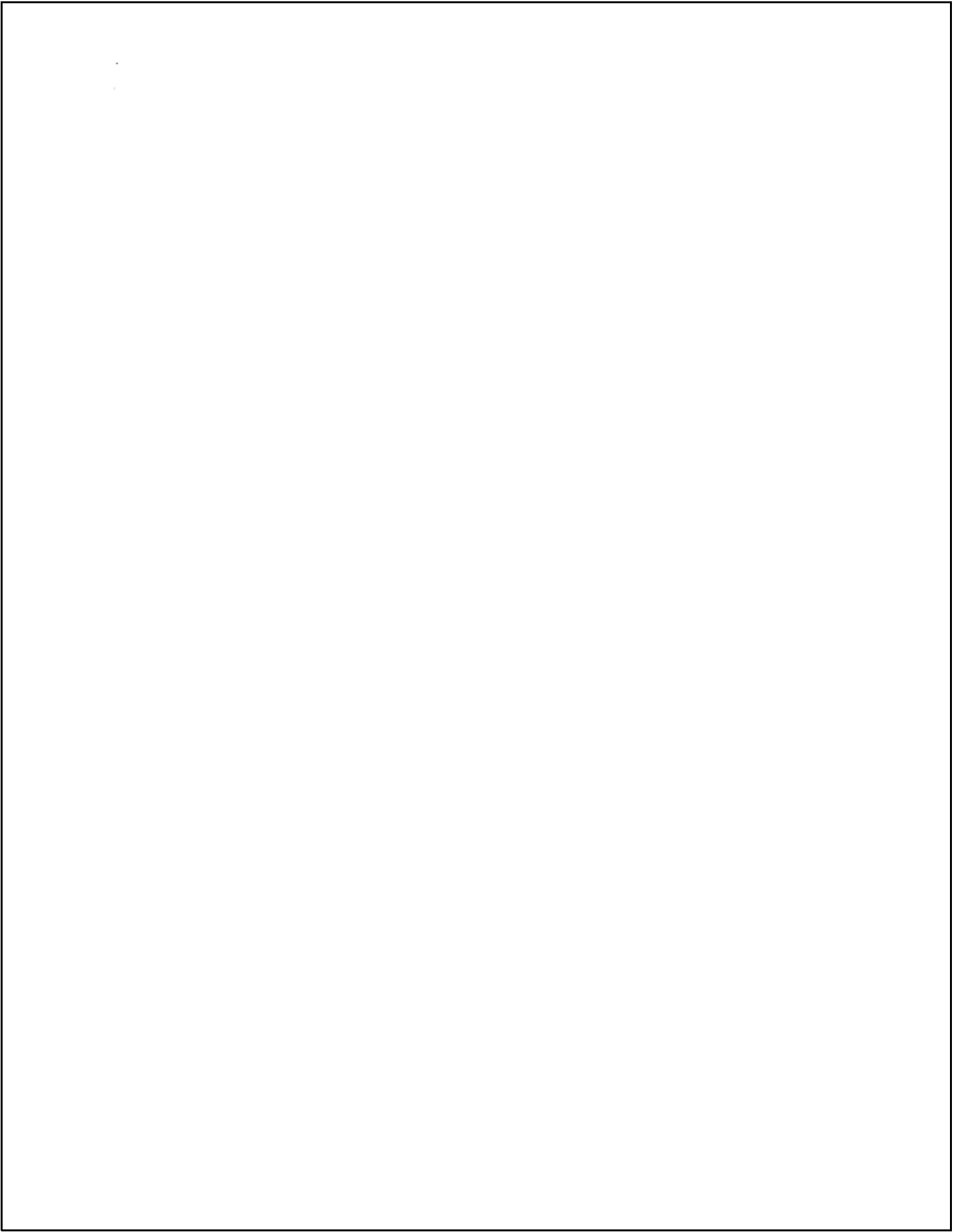
MACQUARIE University
SYDNEY·AUSTRALIA

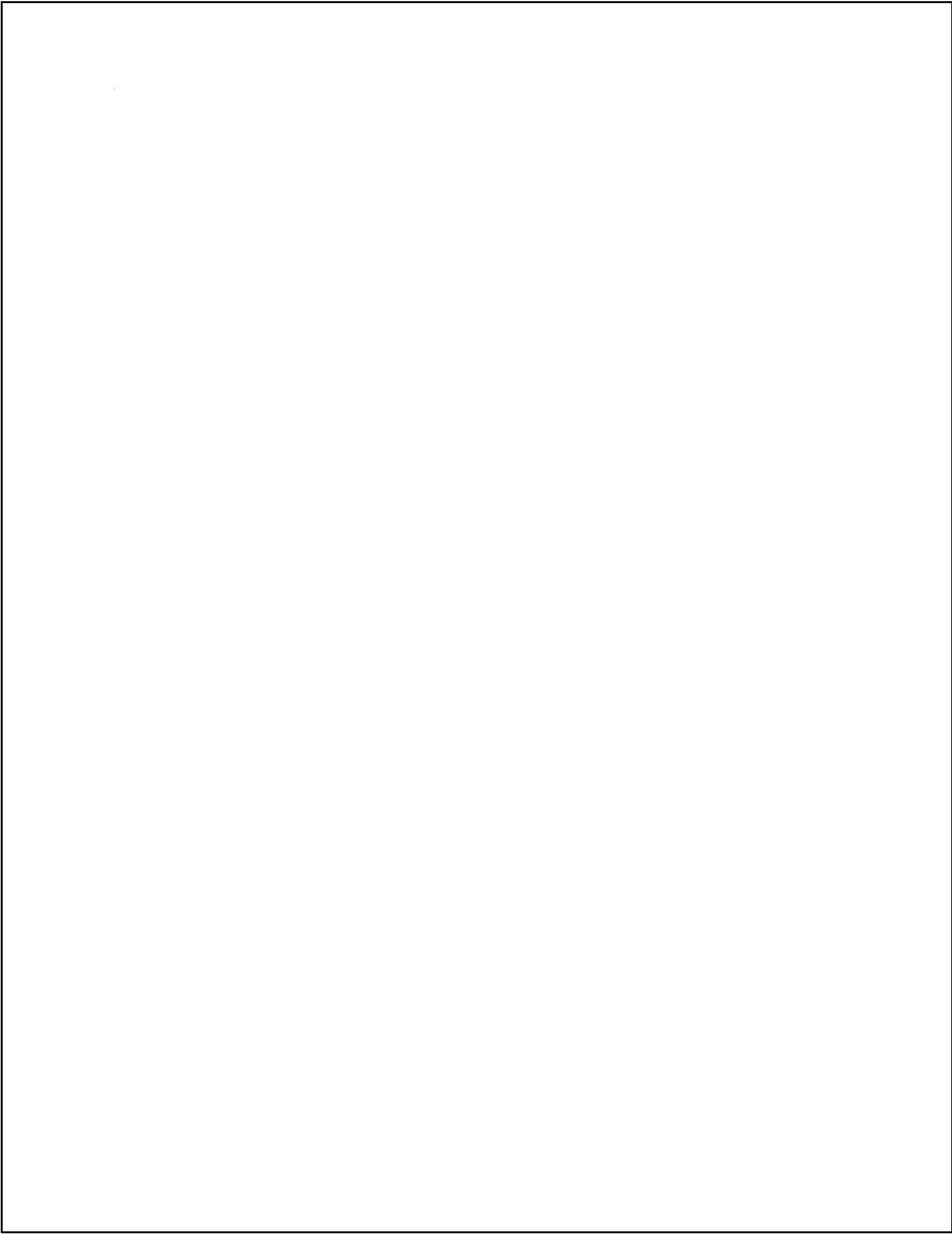Department of Engineering
Macquarie University

November 7, 2016

ACKNOWLEGEMENTS

I would like to express my gratitude to my thesis supervisor Dr Agisilaos Kourmatzis for the knowledge and guidance offered throughout the entirety of this thesis project at Macquarie University.

STATEMENT OF CANDIDATE

I, Sean Fitzgerald, declare that this report, submitted as part of the requirement for the award of Bachelor of Engineering (honours) in the Department of Mechanical Engineering, Macquarie University, is entirely my own work unless otherwise referenced or acknowledged. This document has not been submitted for qualification or assessment at any other academic institution.

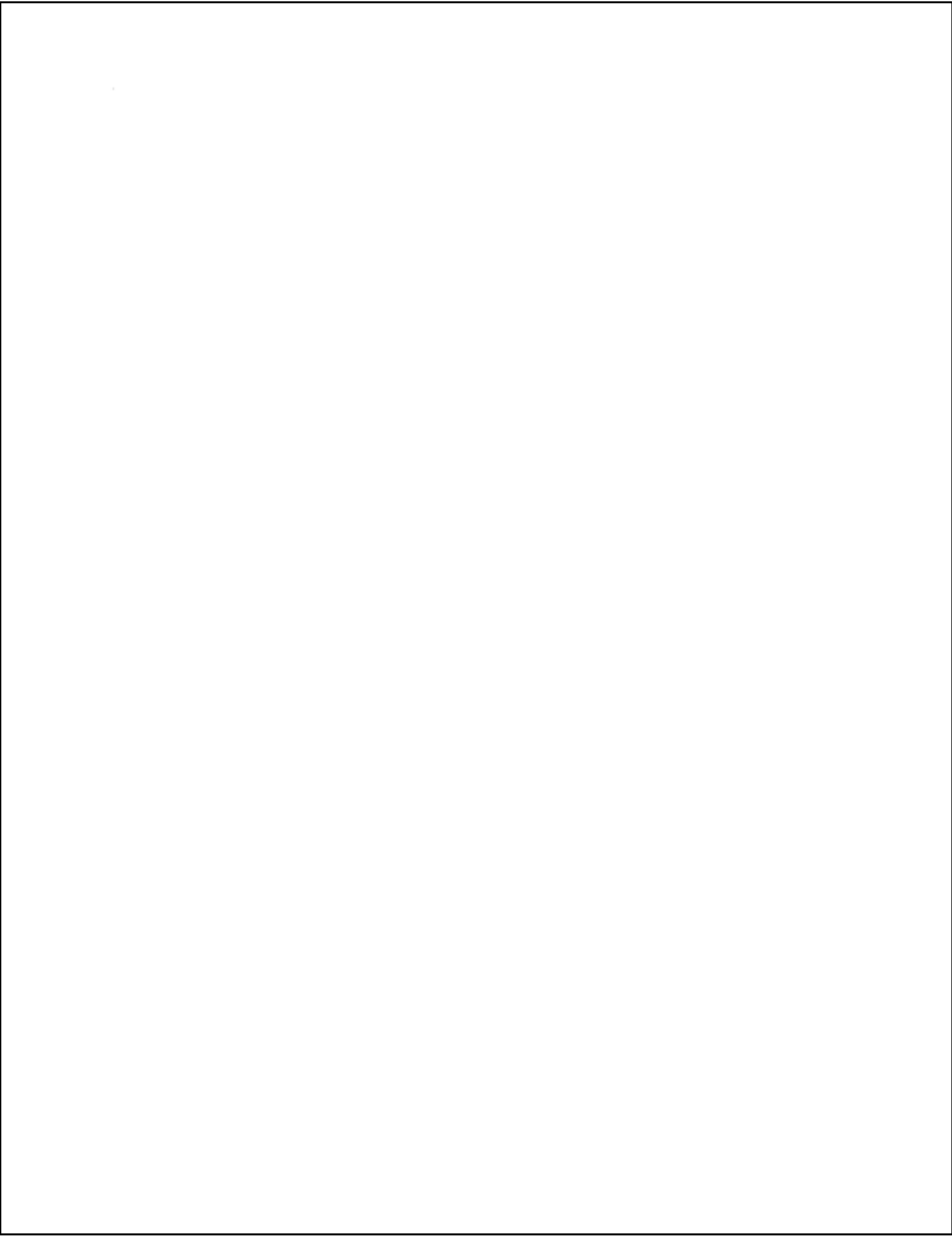Student's Name: Sean Fitzgerald

Student's Signature:

Date: 7/11/2016
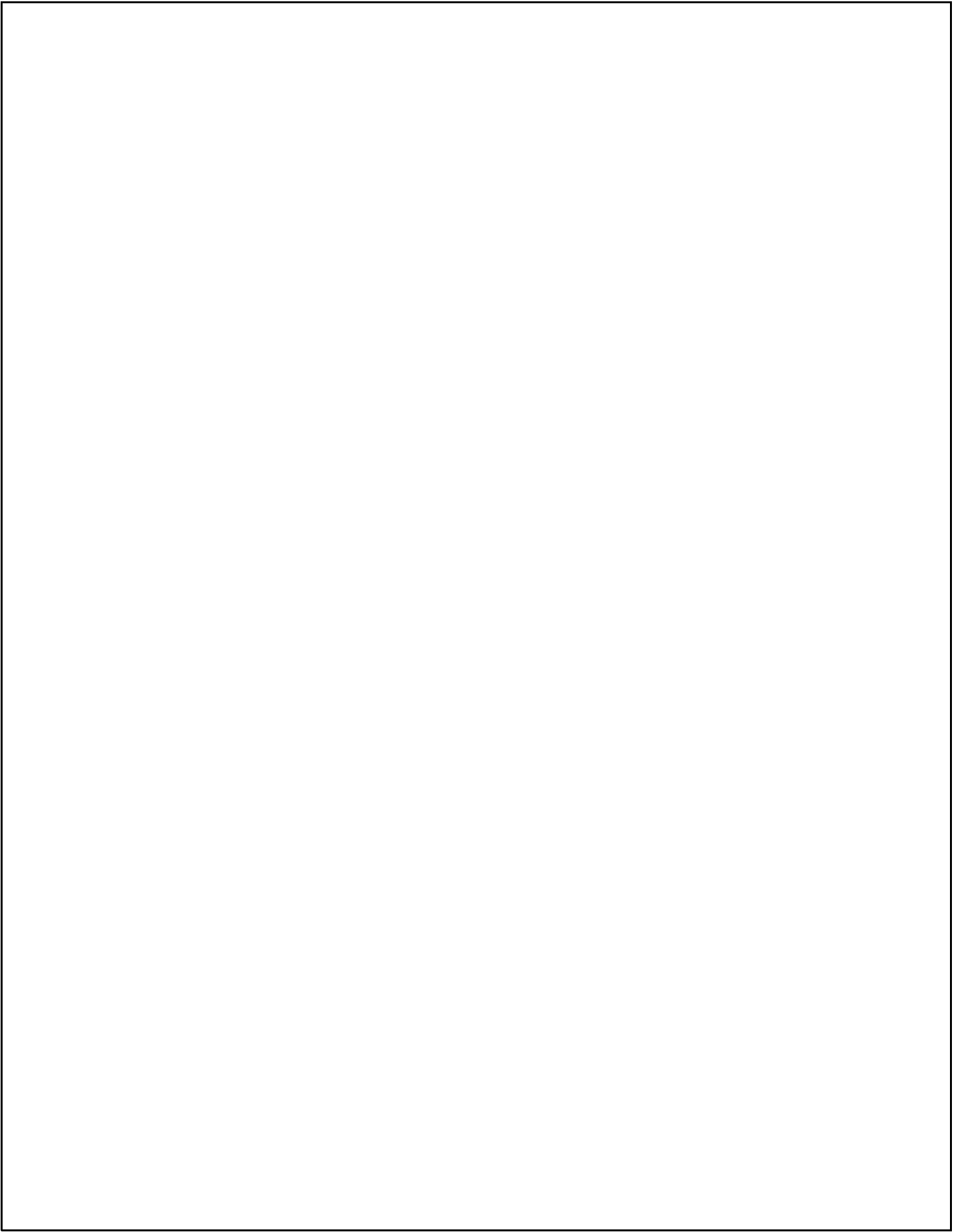
ABSTRACT

The physical parameters of the human cough and sneeze, and how they affect the transmission of pathogens through the air still remains relatively unknown. This fact when considering the affect airborne transmission of disease has had over the history of mankind is astonishing. This thesis intends to provide further understanding of the flow characteristics within the human upper respiratory tract, in conjunction with the design of a coughing machine to reliably reproduce the human cough for medical research. A result of the time sensitive nature of this report, a focus has been set to the airflow with the upper respiratory tract during a cough via 2D simulation. The results gathered through computational fluid dynamics (CFD), identify key flow patterns and enable future iterations of the coughing machine to be refined; producing results closer to that of a human cough. It is hoped that this project will lead to the creation of a coughing machine that can be used in research of the different physical parameters of the cough, and what affect these have its outcome and transmissibility.

Contents

List of Figures

Chapter 1

Introduction

The transmission of infectious disease has been a prevalent issue throughout history, epidemics sweeping across continents with the ability to spread across any country and cripple even the most powerful economies (such as 1918 Spanish Flu causing more than one billion infections) [1]. The human cough and sneeze are one of the most widespread forms of transmission of such disease, with the violent expiratory events releasing pathogen bearing droplets upon unsuspecting victims. Although there have been vast improvements in vaccines and procedures to reduce the risk of transmission. What exactly changes the effectiveness of transmission, specifically for the cough and sneeze is still relatively unknown. The ability for disease organisms to evolve very rapidly produces major complications when developing vaccines, leaving the transmission of even the common flu still a demanding issue within current society.

In order to reduce possible transmissions or nullify the effectiveness of transmission, the development of knowledge around the human cough and sneeze is essential to understand how each mechanism interacts with the overall droplet distribution, allowing further developments for transmission reduction in the future.

Understanding the critical physical parameters with regards to its fluid dynamic properties is the fundamental goal of this project. To accomplish this, ANSYS computational fluid dynamics (CFD) tool FLUENT, will be used to reproduce the human cough via a 2D computer simulation which will allow us to adjust different boundary conditions as observe its effect on the resulting cough.

From the results obtained, the input values used for the simulation can be integrated with another project running concurrent on the same topic. Joshua Scrivener's project is to construct a machine that can replicate the human cough, and apply the simulation data gather into a real life application. The simulations will be used to validate the coughing machine to obtain if it is correctly reproducing a cough, similar to that of the average human.

Current literature (discussed in this literature review) presents many different aspects relatable to this project, but the transmission mechanisms of even the most common respiratory diseases remain poorly understood [2], [19].

1.1 Project Scope

The intention of this thesis is to enable a further understanding into the flows that occur in the human upper airway. This knowledge is to be used in conjunction with the coughing machine to replicate the human cough, and in the future, be implemented into medical research for transmission reduction.

1.1.1 Project Objectives

The following are the set project objective:

- Research the different physical characteristics of the human cough to be able to collect reliable simulation data.
- Create a CAD model of the human upper airway to be implemented in CFD simulations.
- Run CFD simulations to understand the flow experienced in Joshua Scrivener's coughing machine.
- Integrate velocity data collected from simulations into Joshua Scrivener's physical testing for validation.

1.1.2 Deliverables

The following are the expected deliverables of the project:

- Geometry of the human upper airway.
- Flow characteristics of the upper airway from CFD simulations of human cough.
- Research data to be implemented in the coughing machine (Joshua Scrivener)
- Research report on the flow characteristic of the human upper airway during a cough, and how this can be implemented into the coughing machine.

1.1.3 Time Management

To ensure that all set objective and deliverable are achieved, an initial schedule has been established. This schedule has been set to maintain the projects trajectory and insuring its completion by the its due date. Each of these key tasked are covered in detail in Chapter 3: Methodology. The following Table 1.1 and Fig 1.1 display the major project tasks and milestones to be completed during the projects life span.

TASK	Start date	End Date	Duration (days)
Background Research	1-Aug	29-Aug	28
CFD Training	8-Aug	5-Sep	28
Literature Review	21-Aug	5-Sep	15
Progress Report	21-Aug	5-Sep	15
CFD setup testing (simple pipe geometry)	5-Sep	19-Sep	14
Create CAD model of upper airway	19-Sep	26-Sep	7
CFD simulations on upper airway geometry	26-Sep	24-Oct	28
Analyse Results	24-Oct	7-Nov	14
Thesis Document	24-Oct	7-Nov	14
Presentation and Poster	7-Nov	14-Nov	7

Table 1.1 – Project Schedule
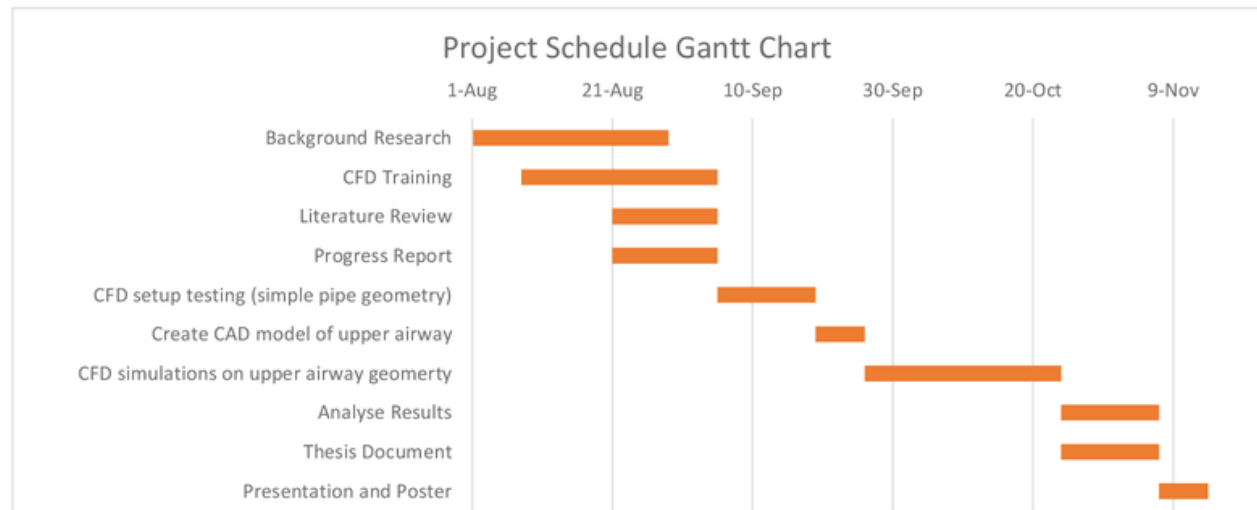
Figure 1.1 - Gantt Chart of Project Schedule

1.1.3 Resources

The equipment required for this project access to a computer with the appropriate Engineering software to run CFD simulations, ANSYS workbench and CREO parametric. This is available on site at the university in the engineering labs E6A 210/211. Some simulations are also run on the student version of ANSYS workbench on my private laptop. All necessary equipment needed to undergo this research topic is already supplied by the university, therefore no extra equipment will be need to complete this thesis.

1.1.4 Cost

As stated in the previous section, all necessary equipment to complete this research topic are already available within the university. Consequently, this project has no costs within the current timeframe, with only minimal costs projected for future works including test equipment and 3D printing. The prescribed budget for this project under the ENGG411 unit is $400, but since that is not required for this application, the funding has pool with Joshua Scriveners concurrent project, where the budget for the coughing machine will be increased to $800.

1.1.5 Risk Assessment

The entirety of this project will be conducted at a computer, because of this there are minimal risks association. The following are the risked associated with this project and the controls setup to combat said risks [24].

Task/Scenario	Hazard	Associated Harm	Controls
Working with computers	Ergonomics: • Repetitive movements • Poor posture • Glare • Long durations in seated position	• Physical injury to wrists, arms, neck, shoulders or back. • Eye strain	• Online ergonomics course complete during ENGG400 • Adjustable chairs and ergonomic designed desks • Routine breaks to reduce the likelihood of injury
Working with computers	Electrical	• Fire • Electric shock • Tripping	• Safety inspections/monitoring of electrical equipment. • Fire safety course complete during ENGG400 • Concealed wires and cords to negate trip hazards.
Working inside a Building	• Trips slips and falls • Fire	• Physical injury • Burns smoke inhalation	• Regular fire safety inspections • Fire safety course complete during ENGG400 • Building safety/fire warden.
Working with people	• Physical/emotional intimidation	• Physical or emotional injury	• Workplace bullying policy • University counselling

Table 1.2 – Associated Project Risk

Chapter 2

Background and Related Work

2.1 Modes of Transmission

The cough produces three types of transmission between the carrier and recipient which have been postulated in medical literature. Aerosol transmission, Self-Inoculation and Large droplet transmission, each are not mutually exclusive [2]-[4]. The mode which is believed to have the most impact of the three is aerosol transmission.

2.1.1 Aerosol transmission

Aerosols by definition are suspensions in air (or in a gas) of solid or liquid particles, small enough to remain airborne for prolonged period because of their low settling velocity [4]. The settling velocity in still air can be calculated using stokes' law [5]. When considering the human cough, the aerosols are the suspension of tiny droplets released as a "cloud" of tiny particles [3,6]. These small suspended droplets are a form of person to person transmission of pathogens through the air by means of inhalation of the infectious particles.
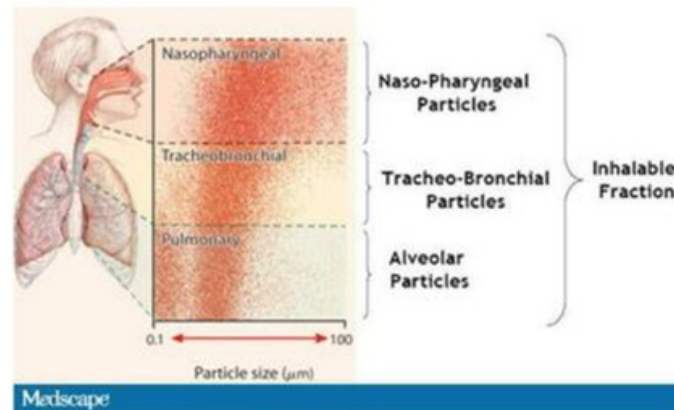
Figure 2.1 - Deposition regions of the respiratory tract for the carious particle sizes

2.1.2 Self-Inoculation

Self -Inoculation occurs when contact is made between the subject and the infectious fluid (be that mucus or other bodily fluids). This is usually a result of close contact with a sneeze or cough, such as someone sneezing behind the subject. Although another example of self-inoculation may be a person coughing into their own hand, now contaminating their hands with contagious nasal mucosa (mucous membrane lining the nasal cavity) [2].

2.1.3 Large droplet

Large droplets are dispelled during a cough, spraying large droplets outward. These droplets would be travelling at a relatively high speed, but would fall to the ground quite quickly and not be suspended for long periods of time like aerosol transmission. This form of transmission is only applicable for short distance transmissions [3].

2.2 Critical parameters

The critical parameters which affect the lethality of the cough are yet to be discovered. In order to allow for this discovery, the variable parameters of a cough must be considered when focusing on the droplet dispersion and deposition [1]:

- Droplet size (μm)
- Mouth formation/geometry
- Airflow velocity (m/s)
- Volume of droplets (L)
- Duration of cough (s)
- Fluid Temperature (^{0}C)

These parameters can be adjusted in both simulations and physical experiments in order to observe whether changing a certain parameter affects the likelihood of transmission.

2.3   Boundary conditions

When solving a CFD case it is essential to define a unique set of boundary and initial conditions. For this project the expected boundary conditions include but are not limited to:

- Inlet - Velocity and volume of fluid released in the expiratory event. During this project, we are only interested in the Velocities, where the inlet velocity will be depended on the outlet velocities required.

- Outlet – Looking at the pressure, velocity and fluid volume released from the mouth. The velocities experienced during a cough can range between 1.15- 28.8 m/s [23]. From these velocities inlet velocities, can be established.

- Wall - possible different temperature from the upper airway (for example the tongue vs roof of the mouth).

Figure 2.2 - Boundary condition positions.

- Time dependent boundary condition – this is and advanced technique allowing different input condition to be varied with respect to time, for example varying the inlet velocity with time.
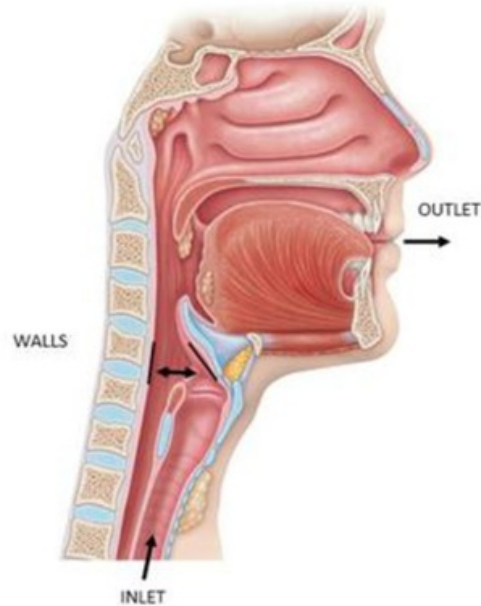
2.4 Droplet size

Two of the main three modes of pathogen transmission via a cough are essentially categorized by their droplet size. Characteristics of dispersion and deposition of the expiratory droplets are highly dependent upon droplet size [1], [8]-[9]. This dispersion and deposition can be predicted in computational fluid dynamics (CFD) simulation. There is an abundance of literature showing droplet size distribution during a cough [10]-[12], sneeze [12]-[13], speech [14] and breath [10] as well as the concentration and number of droplets [11]-[15]. Being able to control the droplet size or testing large droplets transmission results in comparison with Aerosol transmission results would establish which has greater influence on pathogens transmission via cough.

2.5 Mouth formation/geometry

The geometry of the subject's mouth during the violent expiratory event will have a large impact on the other critical parameters, such as the Reynolds number. To understand what effect the shape of the mouth has on these different physical parameters, the geometry would have been me modelled in CAD to mimic the human mouth, and by changing parameters to discover what influence it has on the flow.

2.6 Airflow Velocity

Experimental studies have reported that the exhalation velocity significantly affects the dispersion of droplets and the surrounding airflow patterns [7],[16]. Considerations will need to be made for the initial velocity of the coughed airflow, velocity frequency distribution and velocity distribution in the measurement area, vector and scalar velocities. As stated in the boundary conditions, the inlet velocity is dependent on the outlet velocity and geometry size. From the conservation of energy, the necessary inlet velocity can be easily calculated from selected outlet velocities. The selected outlet velocities will range between 1.15- and 28.8 m/s dependent on what type of velocities are wanted to be tested for the coughing machine (more focus on the higher range) [23]. The velocity at which the body attempts to clear its airways vary between coughs, this would also need to be able to be varied in an experiment of CFD simulation.

2.7 Volume of droplets

The volume-based size distributions of sneeze droplets can be represented by a lognormal distribution function, and the relationship between the distribution parameters and the physiological characteristics of the subjects are studied by using linear regression analysis [1]. The volume- based size distribution is the ratio of the volume of all the particles with the diameters in each size range and the total volume of all the particles with any diameter in the spray. The total volume of the droplets will be varied to establish if the concentration of droplets affects the rate of infection.
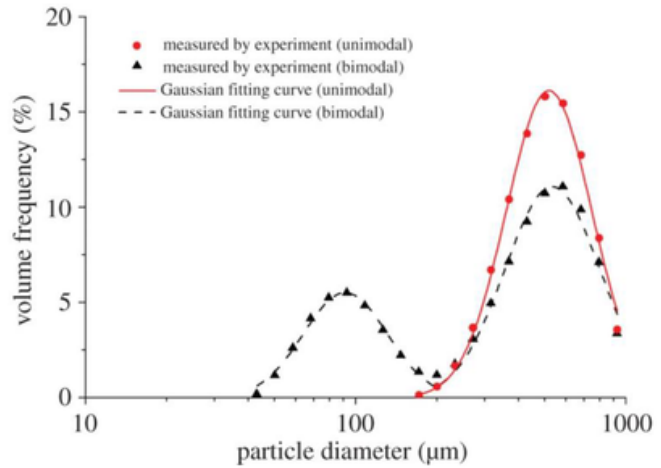
Figure 2.3 -Measured data and fitting curves of two sample sneezes [1].

2.8 Duration of cough/sneeze

For each cough/sneeze, the droplets exhaled at different times through its duration have the same distribution characteristics with good time stability [1].

2.9 Fluid Temperature

The temperature of the fluid and the difference in temperature between the fluid and the ambient temperature will affect the droplet dispersion and deposition. The evaporation of the fluid will also be affected [1],[19].

2.10 Airway Geometry

In order to properly model the human upper airway, the anatomy of the system must first be understood. The airway geometry used for CFD simulations will be focused on the upper respiratory tract, although the nasal cavity at this stage is not going to be pursued as the current focus is on the cough. The respiratory tract is separated into an upper and lower section, with the lower containing the Trachea, bronchi, bronchioles and lungs. The only part of this lower section that will be included in the airway geometry is the Trachea (commonly known as the "wind pipe").

The Upper Respiratory System

Figure 2.4 - Detailed diagram of upper respiratory tract

Essentially the respiratory system is an organism that performs gas exchanges between the oral/nasal cavities and the lungs [28]. The following is a more detailed view of the upper section of the airway which will be represented in the airway geometry.

2.10.1 Pharynx

The pharynx is a cone-shaped passageway connecting the oral and nasal cavities to the esophagus and larynx. The pharynx in usually spilt into three sections: the nasopharynx, oropharynx and laryngopharynx, depicted in Fig 2.5. For this application, the oropharynx and laryngopharynx will

Figure 2.5 - Pharynx

be of interest as the nasal cavity is not being considered at this stage. The pharynx works both as part of the digestive system, as well as he respiratory system. It's main purpose in to transfer food from the mouth to the esophagus, and to filter, warm and moisten air prior to it traveling into the trachea. When swallowing food, the trachea closes and the food moves through the pharynx and into the esophagus. [25]

. 2.10.2 Larynx

The Larynx, commonly referred to as the voice box, is located between the pharynx and trachea. The larynx allows air to be directed through the trachea while also playing a role in preventing food and drink from entering the lungs.

The Epiglottis is the upper part of the larynx, and is one of the most influential features when considering the flow during a cough. This flaplike structure restricts the passageway significantly, which will in turn increase the velocity around this area. This area around the epiglottis is of significant interest as it will most likely produce the largest disturbance to the flow between the trachea and the mouth.

2.10.3 Trachea

The trachea is a cartilaginous tube that connects the pharynx and larynx to the lungs. Its function is to allow air to travel between the nose or mouth and into the lungs. The inlet for the geometry will start at some stage along the trachea, with a reasonably constant diameter [26], it will be a good position for the inlet and can be extended to allow for the flow to become fully developed if required.

2.11 Computational Fluid Dynamics (CFD)

In order to solve the complex fluid flows involved during the human cough, computational fluid dynamics (CFD) has been employed in order to solve said problem via computer simulation. 2D simulations of the human cough are all run using the ANSYS Workbench software package. The software package offers two CFD tools which could be used to solve the given case. The simulations have been run in the FLUENT tool as it offers the use of a 2D solver, allowing for more efficient solution times in comparison to the CFX tool.

2.11.1 Turbulence model

It was obvious when determining whether we would be dealing with laminar or turbulent flow, based on the size of the geometry and high velocity experienced, the flow throughout the upper airway tract would be turbulent. During a study of the human cough, where many samples where taken (n=195), the Reynolds numbers ranged between 2,300 to 57,600 [23]. This would mean that the majority of coughs recorded are turbulent, with a "weak" cough with a very low velocity producing a laminar flow. This was further reinforced by a Reynolds Number calculation in the methodology; finding a value higher than 4000, subsequently defining a turbulent flow for the geometry.

2.11.2 K-epsilon turbulence model

The K-epsilon model is a two equation model that allows for mean flow characteristics for turbulent flow conditions do be simulated. The first variable is the turbulent kinetic energy (k), and the second is the turbulent dissipation (ε) [22].

For turbulent kinetic energy k:

$$\frac{\partial(\rho k)}{\partial t} + \frac{\partial(\rho k u_i)}{\partial x_i} = \frac{\partial}{\partial x_j}\left[\frac{\mu_t}{\sigma_k}\frac{\partial k}{\partial x_j}\right] + 2\mu_t E_{ij}E_{ij} - \rho\epsilon$$

For turbulent dissipation ε:

$$\frac{\partial(\rho\epsilon)}{\partial t} + \frac{\partial(\rho\epsilon u_i)}{\partial x_i} = \frac{\partial}{\partial x_j}\left[\frac{\mu_t}{\sigma_\epsilon}\frac{\partial\epsilon}{\partial x_j}\right] + C_{1\epsilon}\frac{\epsilon}{k}2\mu_t E_{ij}E_{ij} - C_{2\epsilon}\rho\frac{\epsilon^2}{k}$$

These two additional equations allow the model to account for known effects on turbulent flow such as convection and diffusion of turbulent energy.

Some advantages and disadvantages taken into account when selecting this turbulence model [22]:

Advantages:

- Relatively simple to implement
- Stable calculations that converge relatively easily
- Reasonable predictions for many flows

Disadvantages:

- Poor prediction of swirling and rotating flows
- Only valid for fully turbulent flows
- Requires wall function implementation

Chapter 3

Methodology

3.1 Simulation setup – Simple geometry

The setup for the simulations will be done first using a simple straight pipe flow geometry, where the boundary conditions, mesh size and turbulence model can all be established. This allows any issues to be resolved prior to applying these constraints to the more complex geometry of the human upper airway. This setup process will simplify the mesh sizing selection process, as well as troubleshooting errors and issues, by reducing the solution time and overall difficulty with a less complex geometry.

3.1.1 Reynolds Number

A suitable Reynolds number for the simple geometry must be established that will realistically represent that of a human cough. From a study held by the university of Colorado, where 29 subjects had their coughs (total of 195) recorded using particle image velocimetry, providing instantaneous velocities and related fluid properties. The resulting maximum velocities found ranged from 1.15 to 28.8 m/s, with Reynolds numbers ranging from 2,300 to 57,600 [23]. For this application, several Reynolds numbers within this range will be tested on the simple geometry to establish any issue prior to the implementation of the complex mouth upper airway geometry.

The selected Reynolds numbers to be simulated in the simple geometry are 17,000, 30,000 and 40,000. From the Reynold number range specified, this will give a good variety, especially towards the higher end of the spectrum.

3.1.3 Simple pipe dimensions

For the simple straight pipe flow, the diameter and width of the pipe would need to be determined to properly represent a similar scenario expected in the complex geometry. Since the diameter of the complex geometry will fluctuate throughout, the selected diameter will only have to sit within this range as it is only a test case/simulation to enable a smooth setup for proceeding more sophisticated cases. The selected diameter for this simple geometry case is 25mm, the average size of an adult male's trachea [26]. The trachea is the connection between the larynx and the lungs, regarded colloquially as the wind pipe.

To determine the length of the test geometry, the main aim is insuring the flow is fully developed. To do this a geometry was created and velocity profiles taken for every meter to find where the flow becomes fully developed. This geometry sizing setup was done using FLUENT's laminar flow. The graph below shows the velocity profile progression per meter of the geometry.
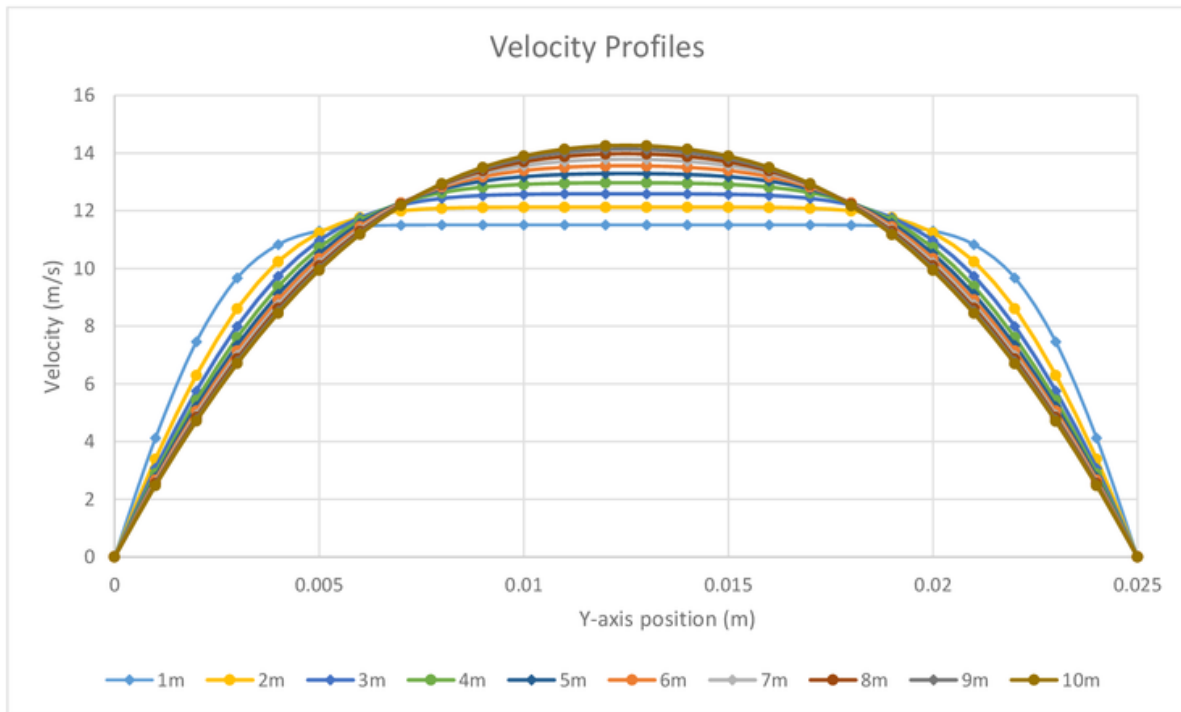

Figure 3.1 - Laminar Flow Velocity Profiles

Eventually at the 10m mark of the pipe, the velocity profile has become fully developed with subsequent velocity profiles converging and overlapping each other.
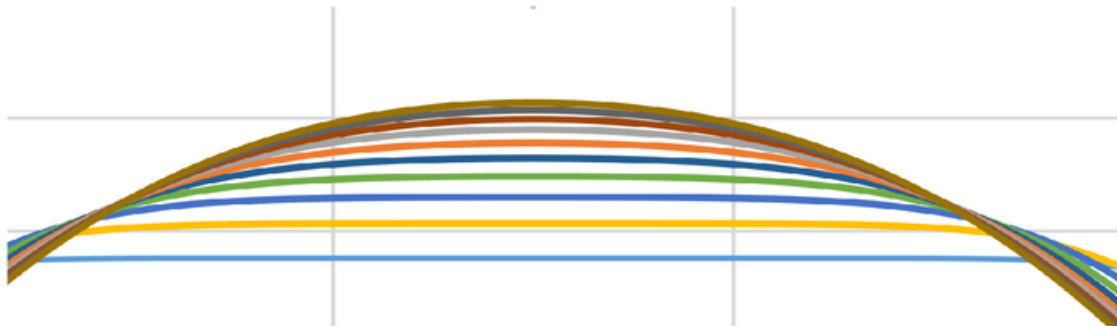

Figure 3.2 - Close-up of convergence in Fig 3.1

The geometry length was chosen to be 15m as it would include a fully developed flow, since steady state simulations are to be used the only critical aspect of this selection is that the flow is fully developed. The final geometry dimensions selected for the simple geometry is a diameter of 0.025m and length of 15m.

3.1.4 Mesh sizing selection

To produce reliable simulations while keeping processing times reasonable (due to the time sensitive nature of this project), a mesh size must be chosen that will allow comparably fast solve times while providing consistent detailed results.

The starting point for choosing a mesh size is calculating the Kolmogorov microscales, which will represent the smallest scale of turbulent flow before it dissipates to heat.

The Kolmogorov length scale will represent the smallest possible mesh size necessary for the given case, but this will almost certainly be unrealistic for this application due to limited computational resources. If such computational resources become available in future works this mesh sizing would be the ideal choice.

Knowing the two extremities of the mesh sizing from one cell to the Kolmogorov length scale, a trade off needs to be made between detail of results and processing time. This decision will be done via the simple pipe flow geometry, comparing the mean velocity against different mesh sizing and finding a sizing that will produce a similar result while solving more efficiently.

Kolmogorov Length scale calculation

In order to arrive at an estimated scale for energy dissipation within the pipe flow the Kolmogorov length scale has been employed to represent the mesh size necessary to fully resolve turbulent flow. Using the kinematic viscosity (v) and the dissipation rate per unit mass (ε).

$$\text{Kolmogorov length scale} \quad \eta = \left(\frac{v^3}{\epsilon}\right)^{1/4}$$

When finding the dissipation rate per mass unit (ε), the largest possible eddies formed are considered as they will account for the majority of momentum and energy within the pipe flow. The size of these large eddies are constrained by the geometry boundary or in this case the diameter of the pipe. Kolmogorov's similarity hypotheses consider these large eddies as the energy source from which smaller eddies are formed. These eddies continue to reduce in size until all structure is lost, at which the energy dissipated by viscosity must be equal to the supplied kinetic energy. Therefore, the dissipation rate per mass unit (ε) can be calculated by accounting for the kinetic energy of the flow (which is proportional to the velocity square, u^2) and the time scale or "turnover" time for the large eddies (which can be estimated as d/u). Giving the following formula [29]:

$$\varepsilon \sim \frac{u^2}{d/u} \rightarrow \frac{u^3}{d}$$

Substituting this back into the original formula gives the formula used to find the Kolmogorov length scale for this case.

$$\eta = \left(\frac{v^3 d}{u^3}\right)^{\frac{1}{4}}$$

$$\eta = \left(\frac{(1.343x10^{-5})^3(0.025)}{10^3}\right)^{\frac{1}{4}}$$

$$\eta = 1.569x10^{-5}$$

Mesh size

When considering the mesh size selection, an optimal cell size was deduced by comparing the cell size to the mean velocity along the center of the pipes characteristic length. The mesh size selected would be that which sacrifices the least amount of accuracy to reduce the order all simulation time. This process was first done with a laminar flow to verify the methodology.
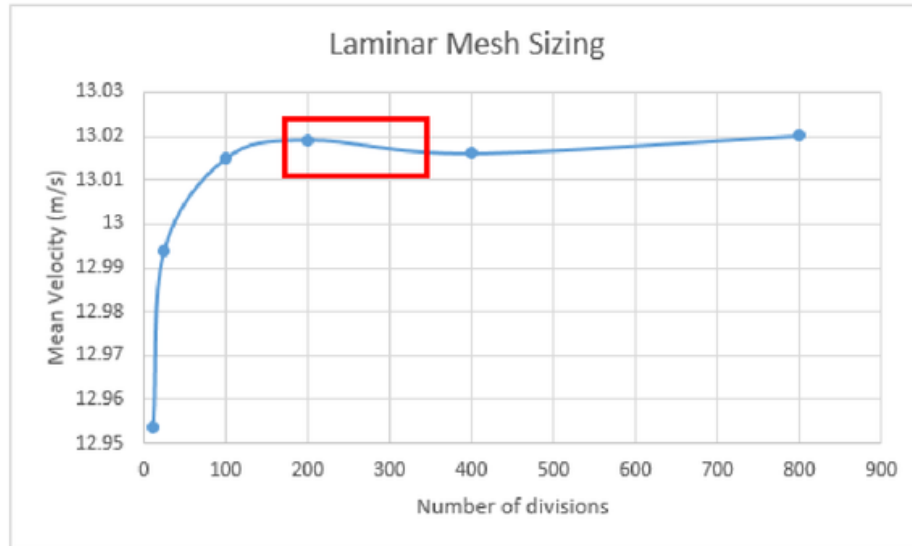

Figure 3.3 - Mesh size with respect to the mean velocity along the centre of the pipe, using a laminar model.

The result has verified that this technique will be able to deduce a suitable mesh sizing for the final geometry. The key region is highlighted in red, contain the most appropriate mesh sizing due to the time sensitive nature of this project. The same testing is then run via turbulence models, since a turbulence model will be used in later simulations.

K-epsilon Turbulence model

The first turbulence model tested was k-epsilon, as it was recognized as the most common choice during the research phase of the project. Although this appears to be the best option regarding turbulence models, the resulting simulation data provided unexpected abnormalities as the mesh was refined. The simulation was run using a Reynolds number of 17,000, which was the first of the 3 Reynolds numbers that would be tested under this method.
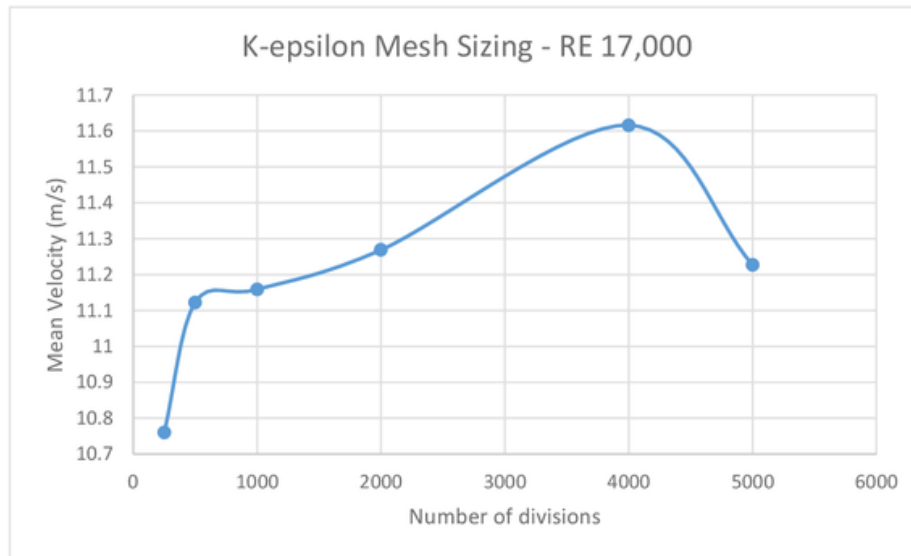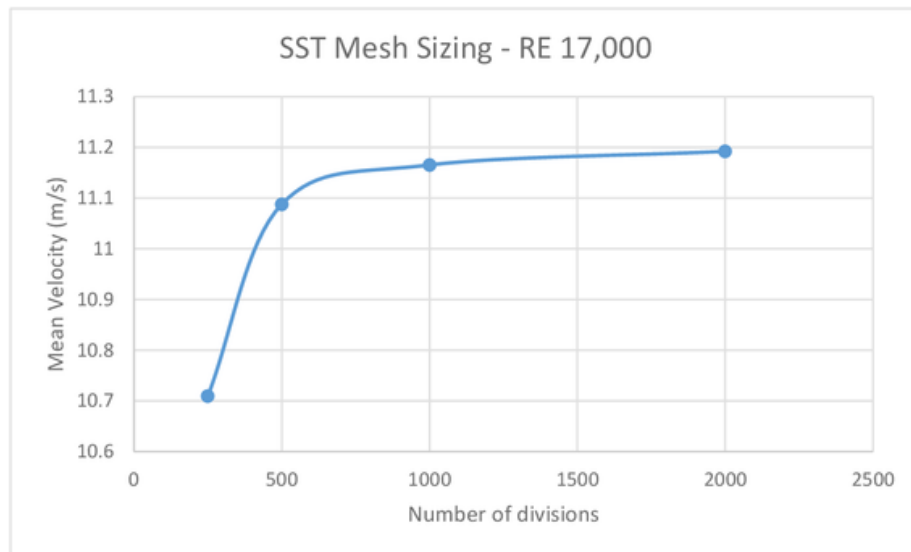

Figure 3.4 - Mesh size with respect to the mean velocity, using FLUENT's k-epsilon turbulence model.
RE = 17,000

The result obtained via the k-epsilon turbulence model clearly differs from the expected profile represented in the laminar results (Fig 3.4). Further simulations where run under different Reynolds numbers and different geometry sizing, all of which gathering similar results. Leaving the k-epsilon models mesh sizing unable to be determined via this method, subsequently another turbulence model would need to be selected or a new method of mesh sizing selection would need to be implemented.

Shear Stress Transport (SST) Turbulence model

The SST turbulence model was to be tested and if a suitable mesh sizing was unable to be established, a new method for mesh size selection would need to be applied. The same methodology was applied to the to the new turbulence model and the following result was obtained.

Figure 3.5 - Mesh size with respect to the mean velocity, using FLUENT's SST turbulence model. RE = 17,000

The resulting profile was exactly as expected and now allows for the mesh sizing to be selected via this method. The ideal choice would be around the 1000-1500 divisions mark, which corresponds to an approximate mesh size of 0.015- 0.01m. The process was then repeated for the remaining two Reynolds numbers (30,000 and 40,000), to observe whether the mesh density necessary will differ at higher Reynolds numbers.
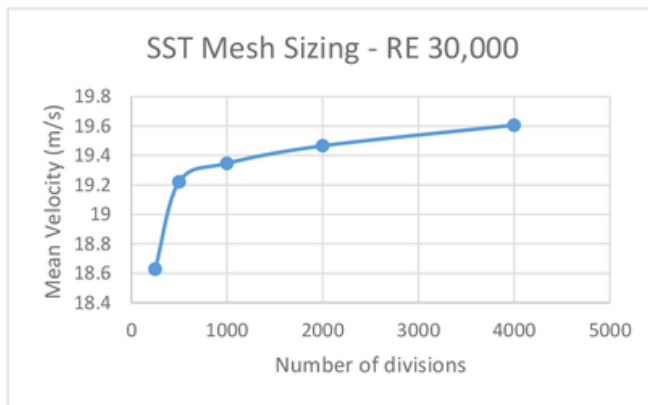
Figure 3.6 - Mesh size with respect to the mean velocity, using FLUENT's SST turbulence model. RE = 30,000
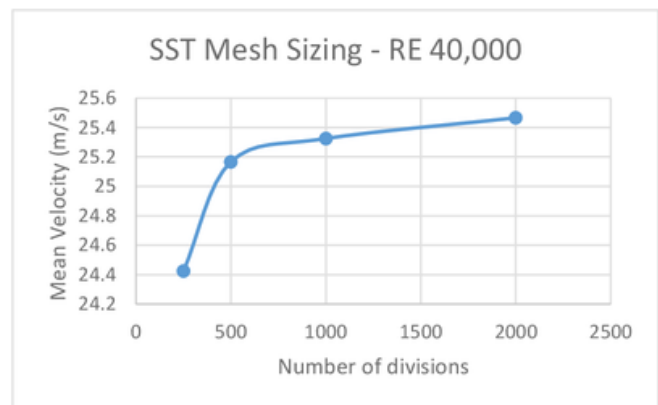

Figure 3.7 - Mesh size with respect to the mean velocity, using FLUENT's SST turbulence model. RE = 40,000

From the three different Reynolds numbers tested it appears that the profiles are very similar, except the difference in velocities makes us unable to compare them on one graph, which would have given the best representation of what mesh size should be chosen. By dividing the mean velocities by their respective inlet velocities, the velocity becomes a dimensionless quantity, thus allowing the three profiles onto be plotted on one graph for comparison.
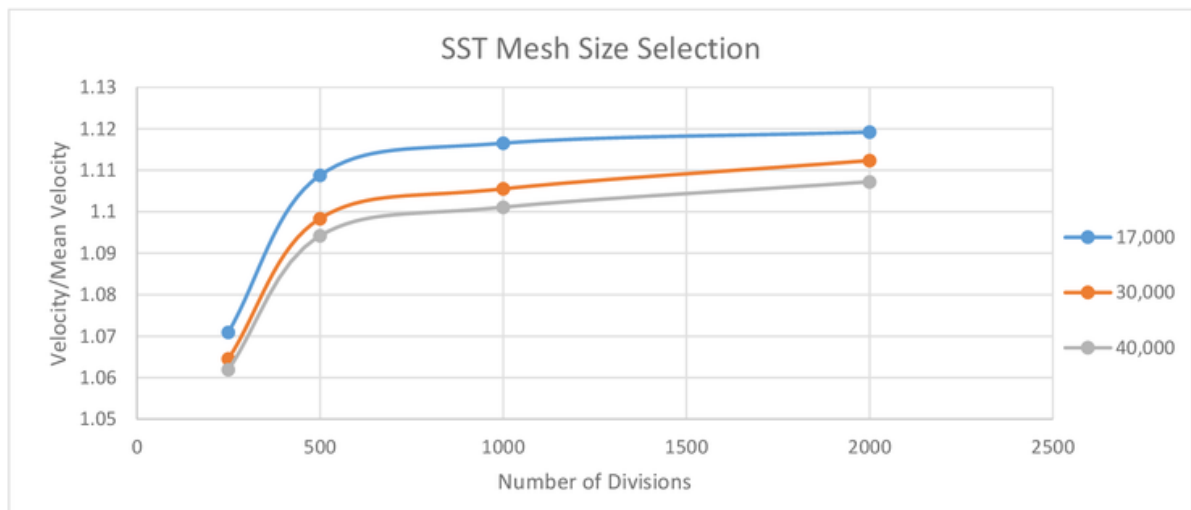

Figure 3.8 - Mesh size with respect to dimensionless velocity. RE = 17,000 , 30,000 and 40,000

From Fig 3.8, it can be verified that a mesh sizing choice of at least 0.015m (1000 divisions) will be necessary, and depending on the solve time for each simulation the mesh could be even further refined. Once the complex geometry in input into the simulation and the solve time is established, further mesh refinement can be made.

3.3   Complex Geometry

A 2D complex geometry will need to be made via CAD software to properly represent the key features of the human upper airway.

From this diagram, we can see that the diameter of this geometry will be constantly changing, with some key areas being the Epiglottis, Larynx and constriction about the tongue. These key features will play a major role in the flow characteristics found in simulations. Therefore, they must be correctly represented within the CAD model, as small changes may have large effects on the CFD results obtained.

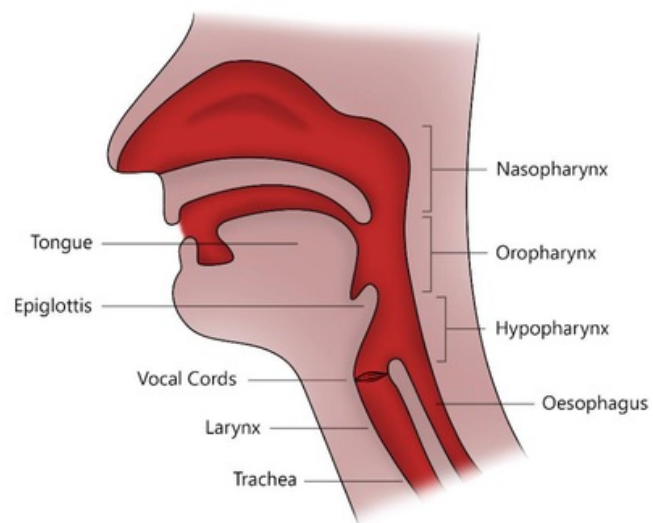The geometry is based on an average adult's upper respiratory tract.

Figure 3.9 - Upper Airway Diagram

3.3.1 Creating Complex Geometry

The method used to create the 2D upper airway geometry, was by using Magnetic Resonance Imaging (MRI) of the upper airway and placing it into CREO Parametric CAD software. This then gave realistic ratio for the entire upper airway. Although the MRI gave good size ratios, it didn't have a scale so the size of it had to be determined another way. The MRI was scaled via research data containing 390 MRI measurement, where the averages of three different positions where found. These three positions where then found on the CAD model and scaled accordingly (marked on Fig 3.10). The following positions where used [27]:

(a) Upper lip length, measured from the stomion superior to the anterior nasal spine
(b) Upper airway width, measured from a point on the posterior outline of the soft palate to the closest point on the posterior pharyngeal wall.
(c) Lower airway width, measured from the intersection of the posterior border of the tongue and the inferior border of the mandible to the closest point on the posterior pharyngeal wall.
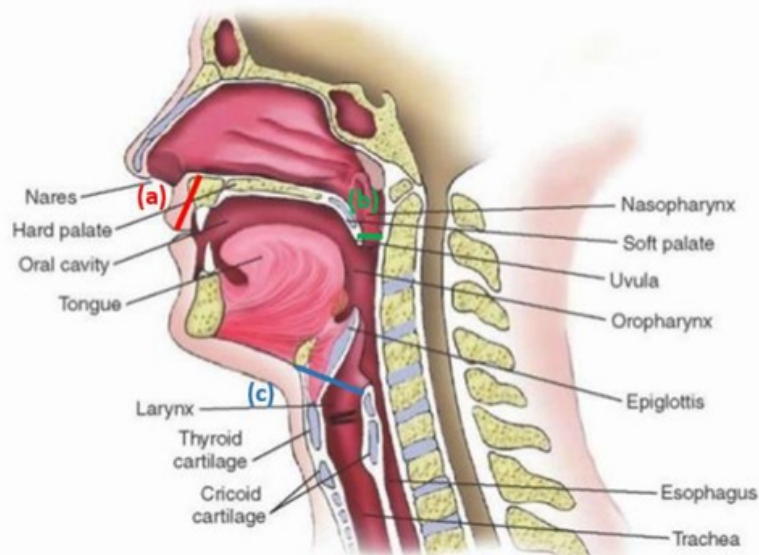
UPPER RESPIRATORY TRACT

Figure 3.10 – Measuring positions used to scale MRI.

These three positions allowed for the MRI to be easily scaled to an appropriate size to represent the human upper airway. The resulting geometry was traced from the new scaled MRI, allowing the new complex geometry to accurately recreate the characteristics of the upper airway.

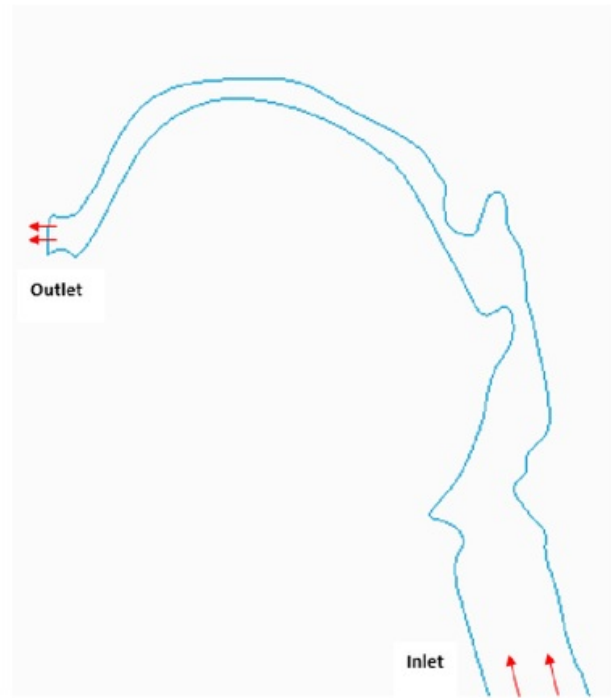Figure 3.11 -MRI of upper respiratory system with 2D geometry overlay

Figure 3.12 - Upper respiratory system

3.3.1 Trachea Length Selection

The inlet position had to be established on the geometry prior to the commencement of final simulations. Optimally the flow would be fully developed prior to the Larynx. To do this the Trachea ("windpipe") was extended, and a test simulation was run to observe how long the flow takes to fully develop, then the Trachea was reduced to this length so the flow would be fully developed prior to the Larynx, while also saving simulation time by having it at an optimal length. This process was completed much like the testing on the simple geometry, where the simulation was run, and the velocity profile could be plotted along the length of the Trachea. Once the velocity profiles have completely converged the flow is fully developed.
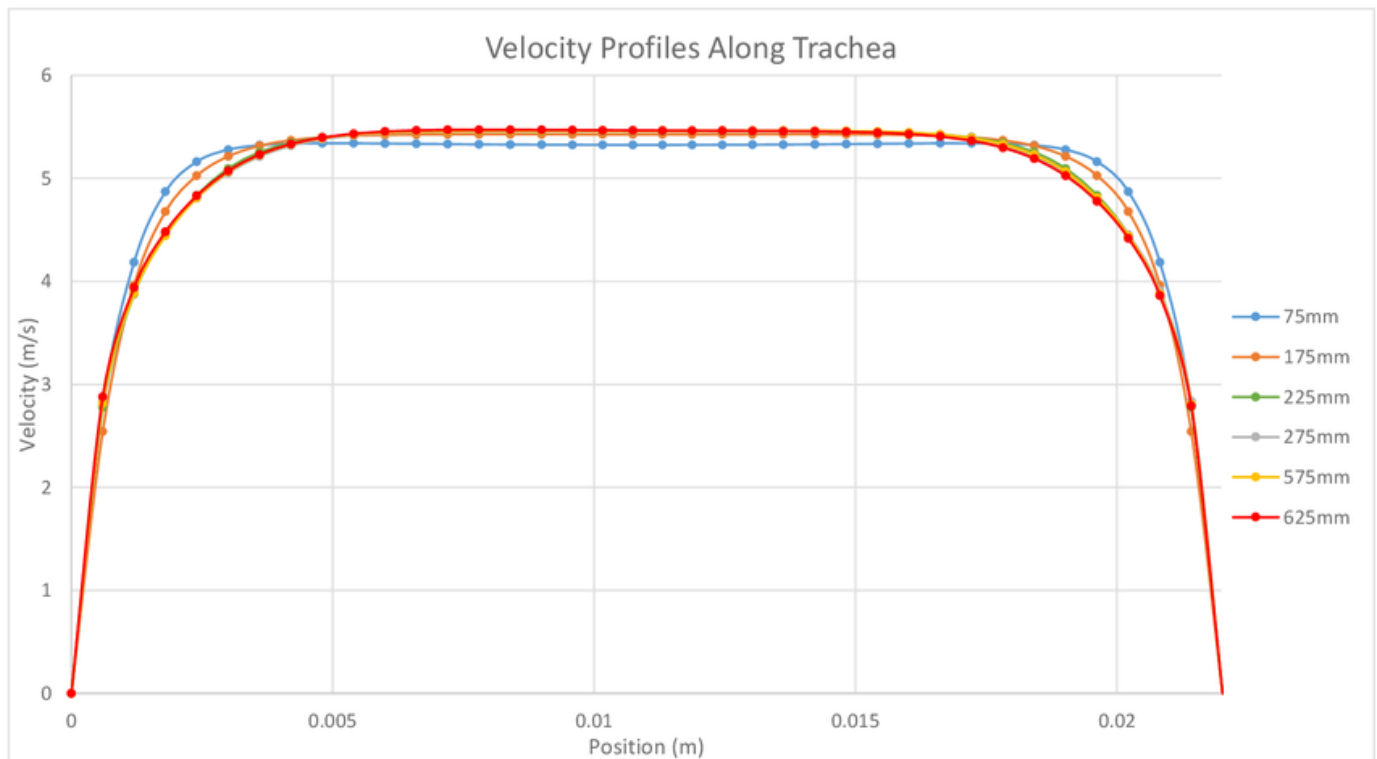
Figure 3.13 - Velocity Profiles along length of Trachea

In Fig 3.13 each group of data plotted is a cross-section of the Trachea, the velocity profile spanning each cross-section is then displayed when the velocities along said cross-sections are plotted. The velocity profile quickly converges from 75mm away from the inlet to 275mm from the inlet. An extra cross-section was made at 225mm to observe whether it was fully converged at that distance, which it also was. It is clear that between 225mm and 625mm the flow is fully converged, and from this a trachea length can be chosen. A trachea length of 225mm was chosen as it is the most optimal choice, as the further the Trachea is extended, the longer the overall simulation will take to solve. Although more cross-sections could be made to find exactly where the flow becomes fully developed, knowing that the flow converges somewhere between 175mm and 225mm. The difference is solution times would be minimal, so the choice of 225mm of Trachea is acceptable since the flow is known to be fully developed.

3.2.4 Integration with Coughing Machine Geometry

The geometry of the coughing machine, made for a concurrent thesis project by Joshua Scrivener, would be implemented to the outlet of the upper airway geometry in order to determine the flow within the mouth geometry. Eventually the upper airway geometry would be converted to a 3D version and used as a replacement for the current straight hose.

The mouth geometry used in the machine consisted of an upper and lower 3D printed mouth section (show in Fig 3.14 in green and red respectively), which is then mounted and held by a support structure. Then a hose was connected via the rear of the 3D printed mouth, where in the future a 3D printed model of the upper airways will be connected.
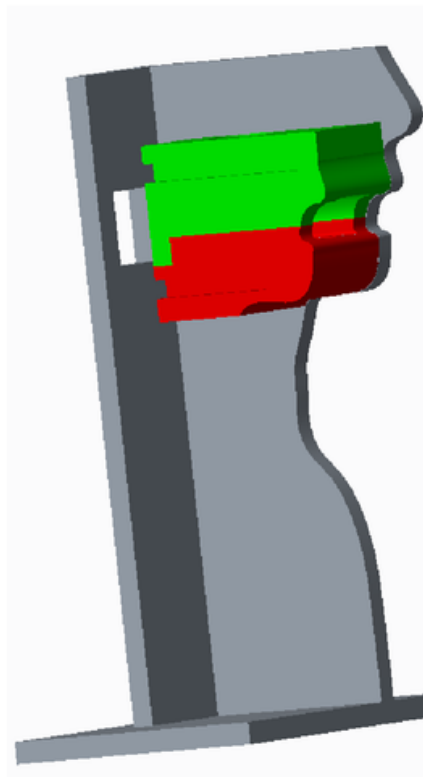

Figure 3.14 - Joshua Scrivener's coughing machine

In order to see what flow characteristic are happening within the mouth geometry; a cross-section must be taken down the center the geometry to convert it to 2D. This now 2D version of the mouth geometry can be connected to the upper airway to complete the complex geometry ready for simulation.
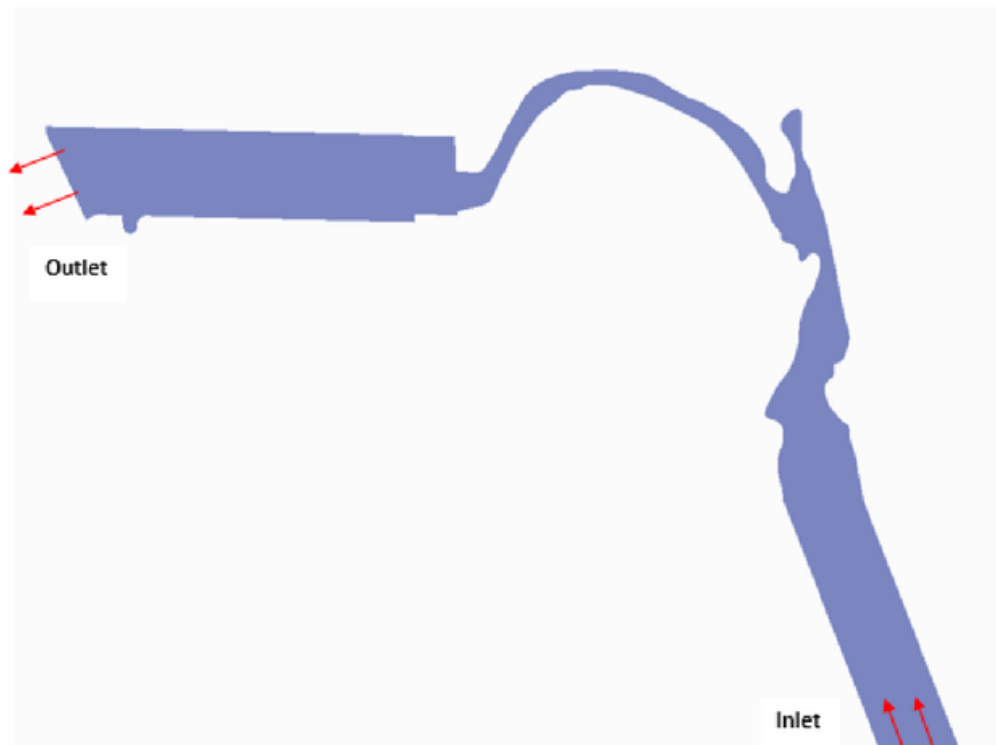

Figure 3.15 - Connection of Mouth cross section and upper airway geometry

This is only the first mouth geometry, where the system has been purposely designed so that new iterations can be 3D printed and directly replaced in the future. This means that the simulation data will directly affect future design refinement of the mouth to enable a proper recreation of the human cough.

3.2.4 Alternative Geometry

Finally, a different upper airway geometry was needed to test its impact on key flow characteristics and eddies formed in the geometry. One major geometry change that can be seen from cough to cough is the jaw placement, with a lower jaw placement opening the airway and a closed jaw restricting it. The second geometry, will simulate a cough with a wider mouth opening, meaning that when the mouth is opened wider the airway is wider above the tongue (since the jaw is lower). This will be an important test as if there is a notable change in the flow, it may be further researched how the mouth position can also change the flow. On top of this, once a 3D printed version of the upper airway is established into the coughing machine, several interchanged geometries could be used in order to replicate different types of coughs.

3.3   Velocity Profile positions for CFD results

In order to gather velocity profiles throughout the upper airway geometry, the points where this data was to be gathered had to be established. The positions chosen will be used to compare velocity profiles between different cases. In total, eight different positions along the geometry where selected, focusing on key regions of interest, especially in the mouth geometry. Since the mouth geometry is already in use with the current iteration of the coughing machine, being able to see how the flow is effected in this region will help with evaluating the best techniques for dispersing fluid like that observed in a cough.

Fig 3.16 displays where these positions are located along the geometry. Each position has be designated a name that all velocity provides are referred to by to reduce confusion.
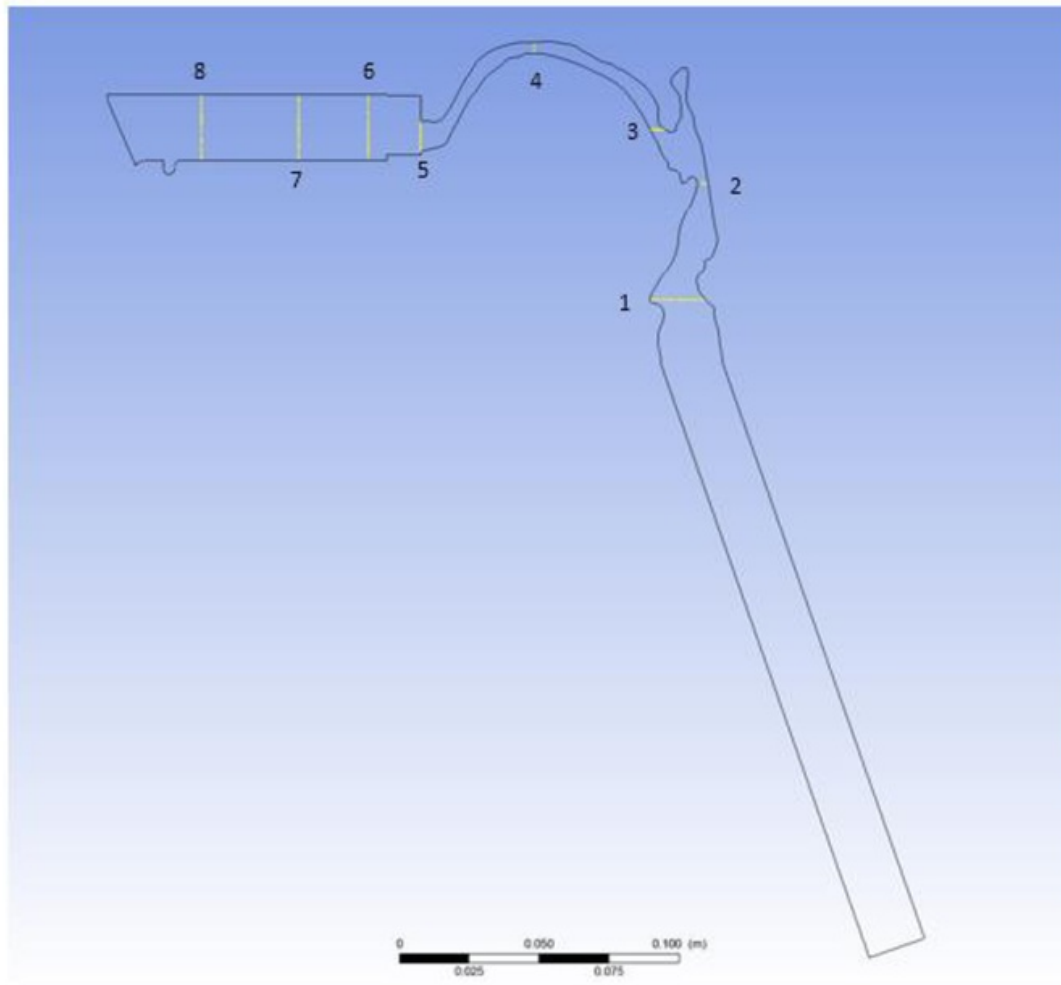
Figure 3.16 - Velocity profile locations

1. Lower Airway
2. Mid Airway
3. Upper Airway
4. Top of Tongue
5. Mouth Inlet
6. Mouth 1
7. Mouth 2
8. Mouth 3

Chapter 4

Results and Analysis

This chapter covers the results from CFD simulations run on the complex geometry of the upper respiratory tract set up in the previous chapter.

4.1 Flow characteristics/formations

The numerical computations are mostly concerned with the flow characteristics and formations that occur in both the upper airway and mouth geometry. Since the respiratory system is complex in shape, a similarly complex flow regime is produced. The aim is to not only understanding how the flow occurs through the upper airway, but also how this flow may affect current and future physical modeling of the coughing machine.

In order to gain a perception of the flow characteristics in the upper airway, velocity vectors have been plotted in Fig 4.1. As discussed during the methodology, the flow enters the model at the inlet and proceeds relatively smoothly as it becomes fully developed. Once the flow enters the larynx and hypopharynx two small recirculating zones on either side of the main flow, shown as point 1 and 2 in Fig 4.1.
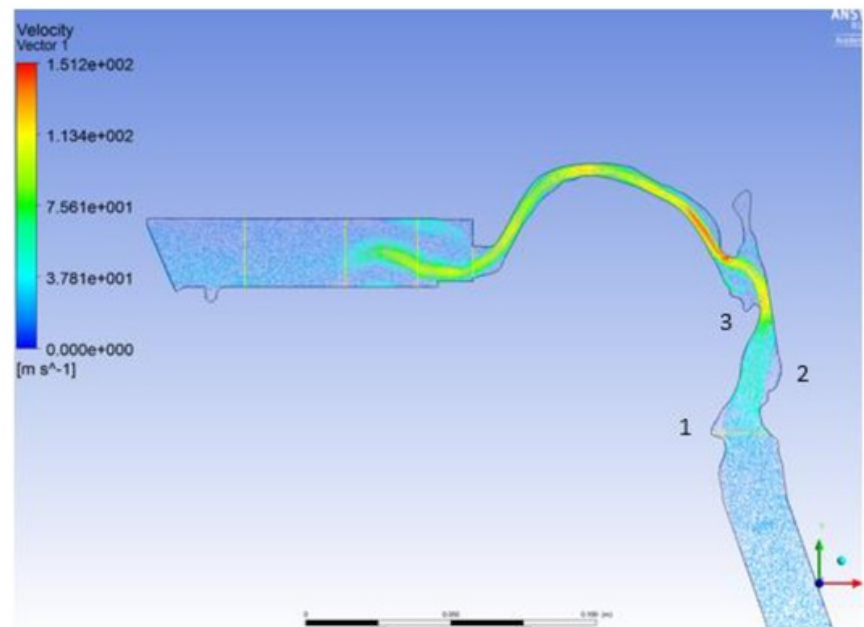
Figure 4.1 - Velocity vectors, SST turbulence model

Past these two small recirculating zones the flow is accelerated due to the restriction of the epiglottis displayed in Fig 4.1 (point 3). This accelerated flow then creates two more eddies either side of the main flow, although these being much larger in magnitude than the previous.
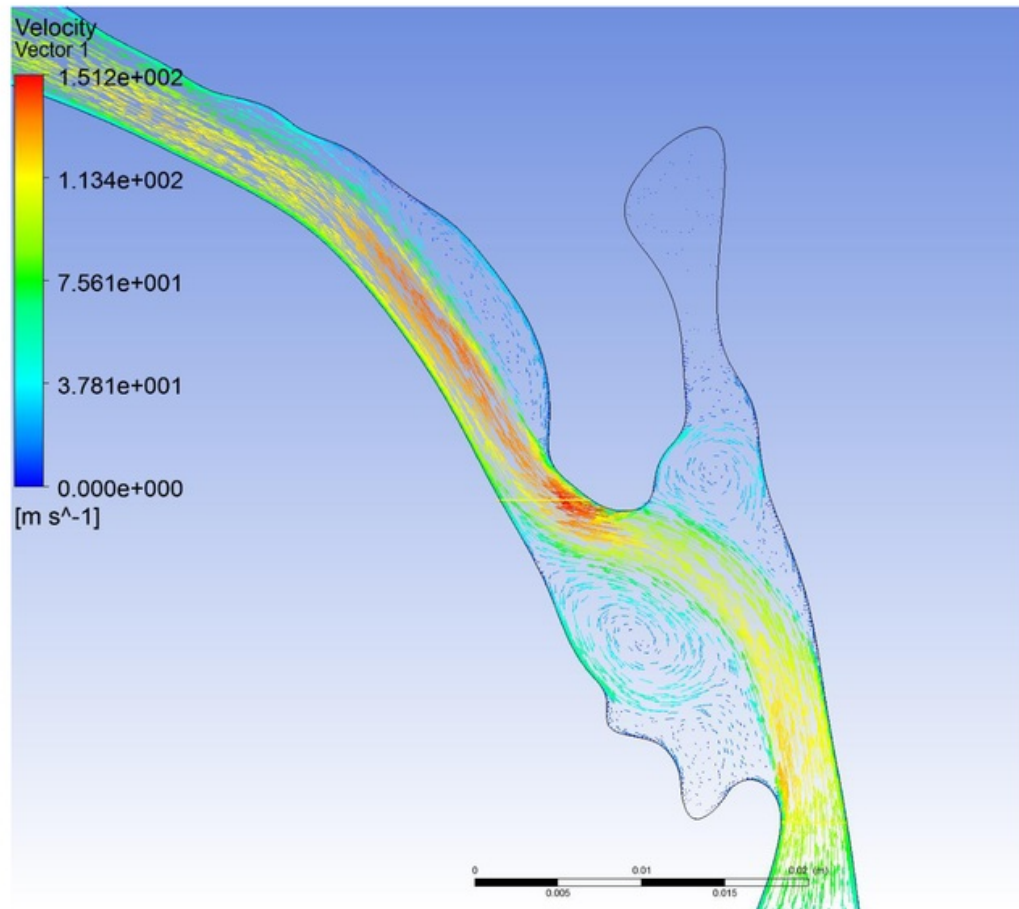

Figure 4.2 - Flow caused by restriction of the epiglottis

These eddies are of importance for future design of a 3D model to be implemented into the coughing machine. These eddies in combination with the narrowing airway induce negative pressures and large wall shear stress, that need to be accounted for in the design of the 3D model to avoid potential model collapse or structural damage. The section shown in Fig 4.2 has the largest concentration of said flow anomalies, and would be a key area of study prior to a physical model being produced.

The flow then continues at high velocity over the tongue, and the flow attaches to the palate (roof of the mouth). Leaving the upper airway geometry and entering the current mouth geometry for the coughing machine. In the mouth geometry, there are two more eddies formed (Fig 4.3 points 4 & 5). The current method for the coughing machine is a thin layer of fluid along the bottom of the mouth geometry. From this data, and future simulations the dispersion of the fluid can be better understood and hence more controlled in future mouth geometry methods. The eddy at point 5 is of interest as this is where the fluid is set for testing. This may cause the fluid to be more evenly distributed across the outlet, whereas if there was no eddy present the fluid would predominantly exit via the lower half of the outlet. This is important to consider in future simulation when mucus fluid can be introduced, where at the moment since we are only addressing the air flow we can only predict what effect this will have on the fluid layer.
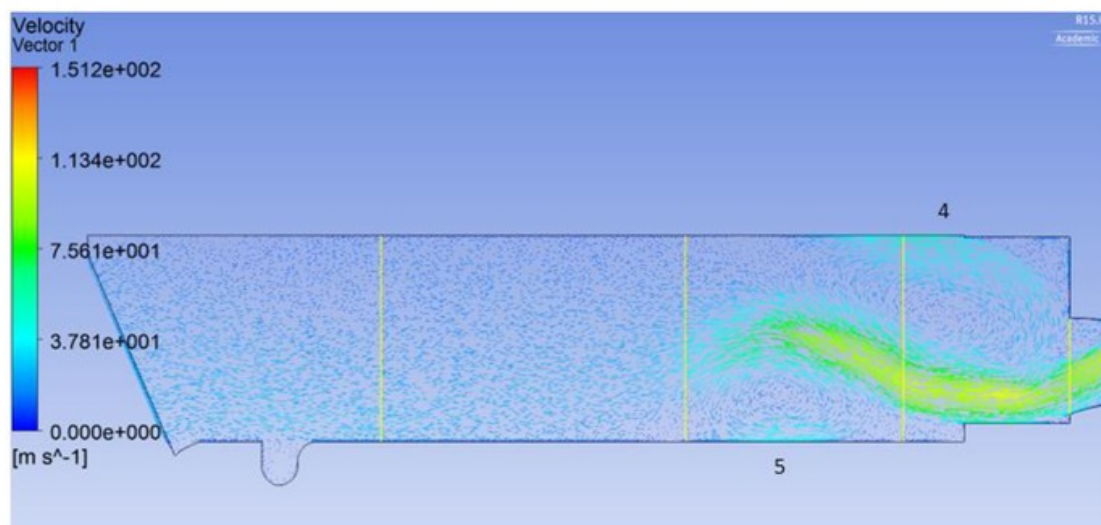
Figure 4.3 - Flow in mouth geometry

The current flow expulsion given by the velocity profile at the outlet can give some insight into how the flow is being distributed from the current mouth geometry for the coughing machine. From Fig 4.4 the velocity profile is fairly evenly distributed, which slightly more focus towards the bottom of the outlet. This is result is good for the fluid distribution since the fluid is contained at the bottom of the geometry. For future iterations of the coughing machine, closer research and testing will need to be done into how the flow is distributed out of the mouth during a cough to be able to replicated this more closely with the coughing machine.
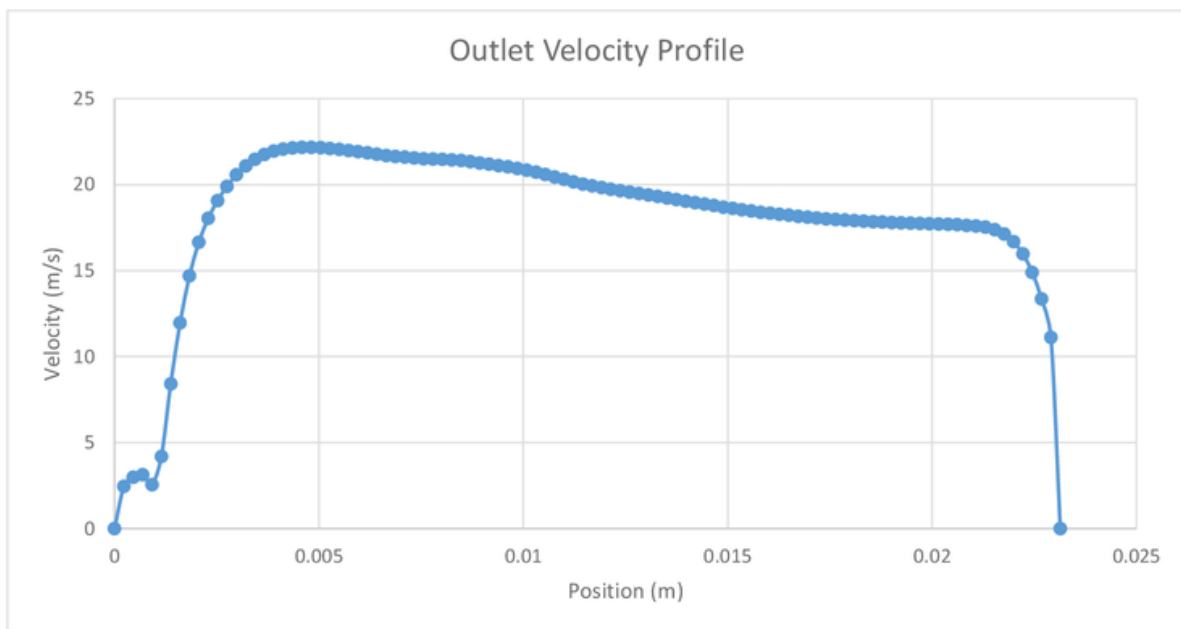
Figure 4.4 – Velocity profile at outlet position

The main flow can be depicted via streamlines in Fig 4.5. Currently this result isn't very useful, but for future research into the fluid placement and different fluid distribution techniques. It shows where the main flow is within the upper airway, as specifically how it behaves in the coughing machines mouth geometry.
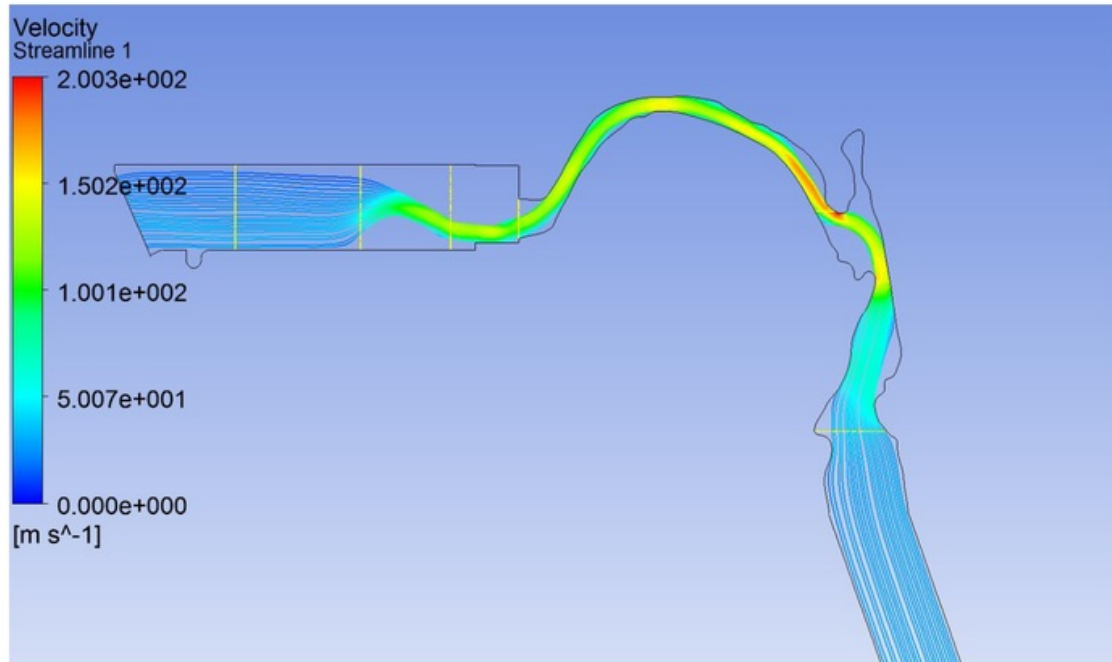
Figure 4.5 - Streamline of flow for RE of 40,000

4.2 Turbulence model validation

The choice of using the SST turbulence model in the methodology was validated to ensure that the flow characteristics and formations are accurate. To do this, simulations where run on the same geometry using the k-epsilon turbulence model, while keeping the inlet velocity constant (20.5m/s). The flow patterns found in the previous section using the SST turbulence model should be replicated in this simulation, otherwise further testing will be required to ensure the reliability of these results. The two sets of simulations will be compared to find any inconsistencies in the flow, and velocity profiles plotted at significant positions will be compared.
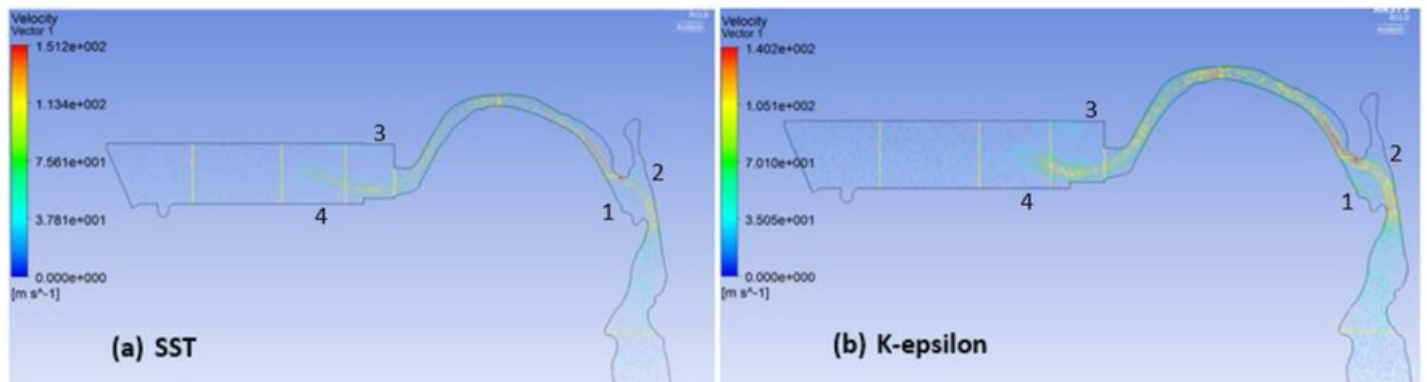
Figure 4.6 - Flow characteristic comparison using velocity vectors, SST vs. k-epsilon

From Fig 4.6, the main flow structures developed in the SST case where all replicated by the verification case using the k-epsilon. These four main points of interested containing the largest eddies are all present in the k-epsilon simulation, and all remain at similar magnitude. The velocity profiles along the eight key points from the methodology were also plotted for each turbulence model and compared to discover any discrepancies.
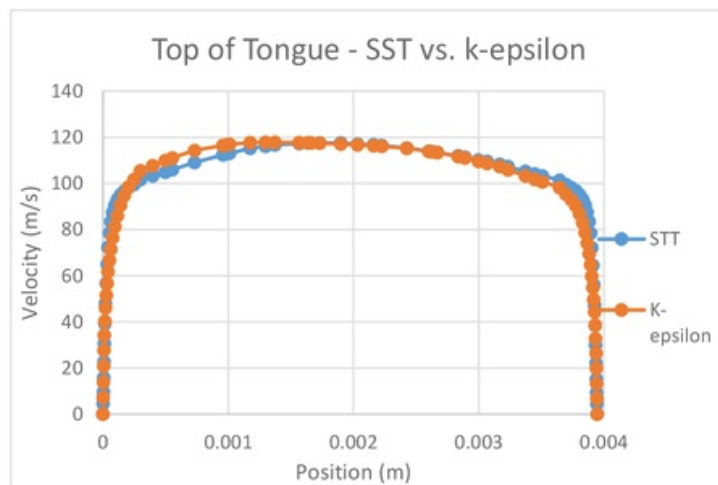
Figure 4.7 - Velocity profiles at the "top of tongue" position for both SST and k-epsilon turbulence models
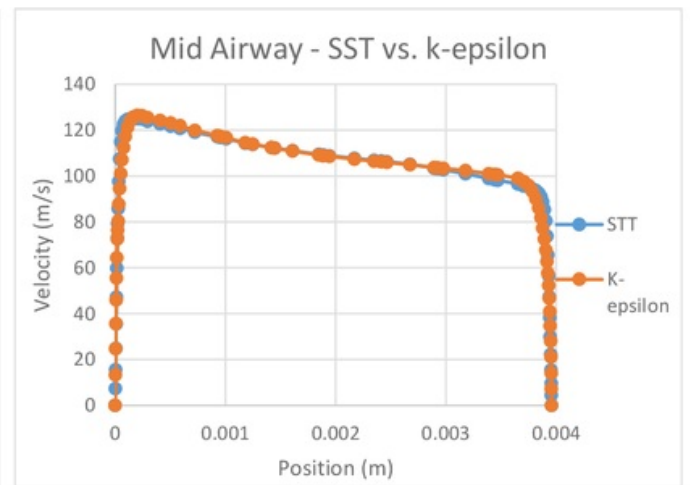
Figure 4.8 - Velocity profiles at the "Mid Airway" position for both SST and k-epsilon turbulence models

The results found from these velocity profiles confirmed the visual inspection of the two velocity vector flows. Only small differences were found in the velocity profile, which could be attributed to a number of causes such as inconsistencies in the mesh. From Fig 4.7 & 4.8, it is shown that these irregularities are minute and overall the velocity profiles gathered are equivalent. This finding therefore authenticates the SST simulation results and flow characteristics.

4.3   Effect of Reynolds number on flow

All previous results where run win a Reynolds number of 30,000. Just like in the simple geometry, the effect of different Reynolds numbers is test to observe how the flow is effected under new conditions. Because of the time depended nature of this project only one other Reynolds number was tested, but ideally a whole range between 4,000 to 57,000 would be tested as discussed in the methodology. Since only one Reynolds number could be chosen, a case was set up for a Reynolds number of 40,000. This Reynolds number is at the higher end of the expected Reynolds numbers to be produced by a cough, and keeps continuity from the simple geometry testing. Both cases were run using the SST turbulence model.

Just like in the previous section, the two cases where compared using velocity vectors to inspect the flow patterns created. Both flows produced eddies in the matching locations, just at different magnitudes as expected since a higher velocity was used for the Reynolds number of 40,000. Since there was no visible variance to the flow, the velocity profiles where once again plotted at the designated key points along the geometry.

Since different velocities are being used, it makes it difficult to recognise if there are any difference in the velocity profiles. To combat this the velocities where divided by their respective inlet velocities to allow for proper comparison (shown in Fig 4.9)
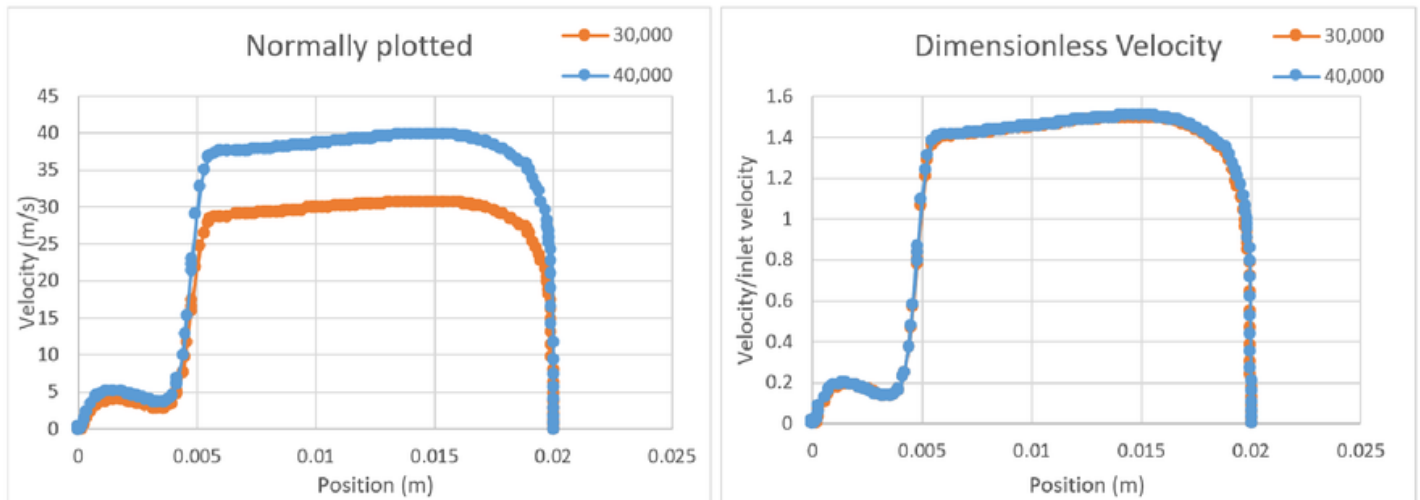

Figure 4.9 - Velocity profiles at lower airway position, RE 30,000 vs. 40,000

This technique was used to compare all geometry profiles. From Fig 4.10 and 4.11 it can be shown that the velocity profiles remained the same under the higher Reynolds number, despite small deviations. Therefore, the flow characteristics where not affected by this change. This may be because the two Reynolds numbers are still relativity close together, and to get a proper conclusion about this the full range of Reynolds numbers would have to be tested in future works.
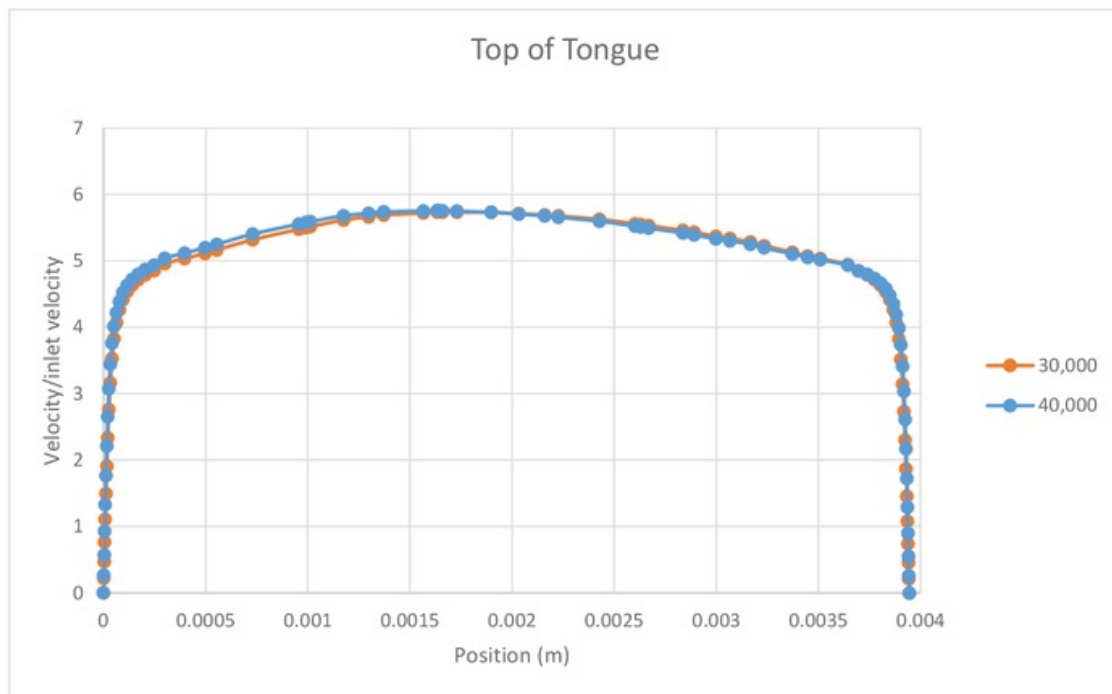
Figure 4.10 - Velocity Profiles at Top of Tongue position for RE of 30,000 & 40,000
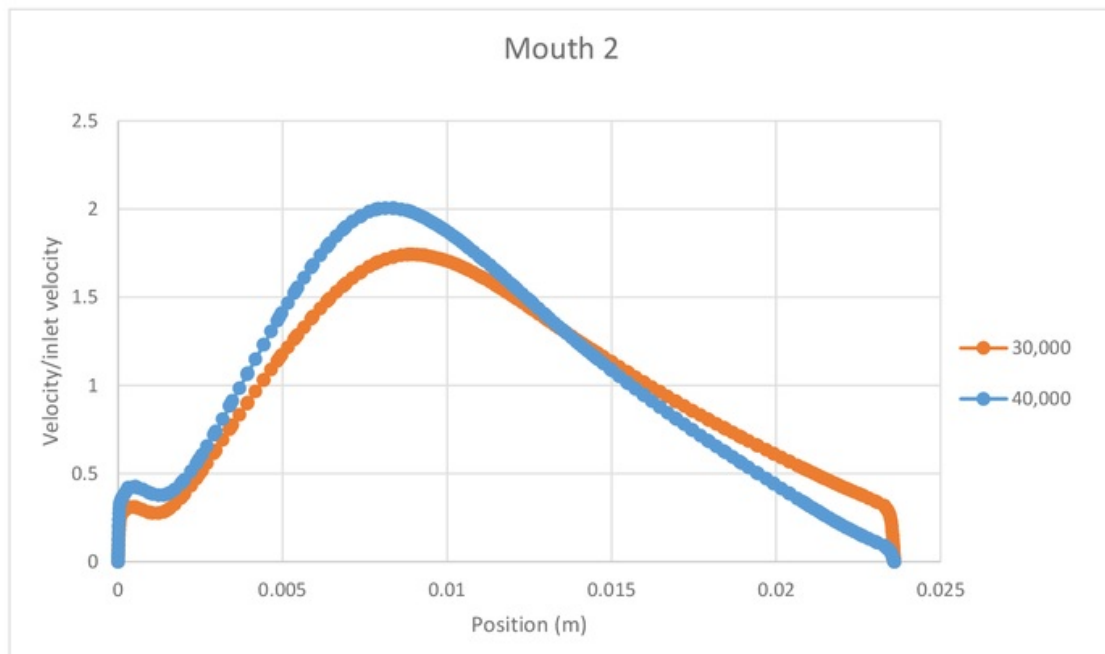
Figure 4.11 – Velocity Profiles at Mouth 2 position for RE of 30,000 & 40,000

4.2   Results Summary

The results gained from this project are predominantly aimed towards future research and development of the coughing machine. Now with an understanding of what is happening within the mouth geometry, the fluid release technique and overall design of the geometry can be reassessed. The main eddies locations and size have been established, with this data the 3D modeling of the upper airway for CFD simulations can now proceed with the eventual goal of replacing the hose that feeds the mouth compressed air; with a 3D printed model of the upper airway.

Chapter 5

Conclusion

The goal of this project was to gain a greater understanding of the flow that occurs in the human upper airway via computational fluid dynamics. During the project the objective moved more towards understand how an upper airway geometry would interact with the current coughing machine, and lay the ground work for the implementation of a 3D printed model of the upper airway to be attached to the machine. To achieve this, simulations had shifted focus from originally an isolated upper airway, to connecting the current mouth geometry to learn the flow patterns prior to the expulsion of the fluid. Also, only looking at the cough; and not the sneeze, therefore the nasal cavity was ignored when creating the upper airway geometry. The results gathered via CFD simulations identify key flow patterns developed in the upper airway and mouth geometry, allowing future designs of the coughing machine to be refined; producing a more reliable recreation of the human cough.

Future Work

The current iteration of the coughing machine in the initial prototype. Through the results gathered by Joshua Scrivener and myself, various design changes and improvements can be implemented to increase the reliability of the coughing machine.

Further research into the cough also needs to be done. Firstly, creating a 3D model of the upper airway via a computed tomography (CT) scan to be analyzed in CFD. From these results a 3D printed model can be created with respect to the forces found via 3D simulation. This will then more reliability recreate the conditions that are undergone during the human cough. There is still a lot of research and testing needed to go into this machine before it can properly recreate the human cough.
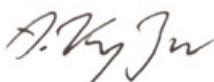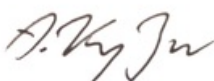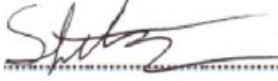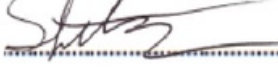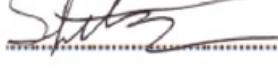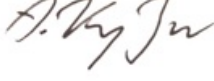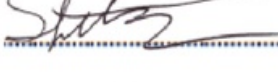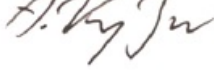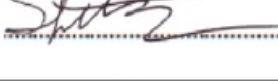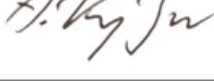
Once the human cough can be reliably recreated, the different physical aspects of the cough, such as droplet dimensions and Reynolds numbers, will need to be able to be varied. By being able to vary each physical parameter, research can be carried out to establish how each of these parameters effect the overall cough, and how this change in cough can affect its transmissibility.
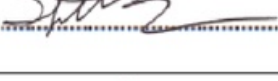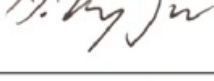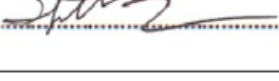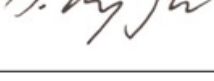
Bibliography

[1] Han ZY, Weng WG and Huang QY, "Characterizations of particle size distribution of the droplets exhaled by sneeze," .J R Soc Interface 10, Jun. 13 2013.

[2] Bourouiba, L., Dehandschoewercker, E. and Bush, J, "Violent expiratory events: on coughing and sneezing," *J. Fluid Mech.*, 745, pp.537-563, Jan. 4 2013

[3] Tellier, R, "Aerosol Transmission Of Influenza A Virus: A Review Of New Studies," *Journal Of The Royal Society Interface* 6, Sep. 22 2009

[4] R. Tellier, "Review of Aerosol Transmission of Influenza A Virus", *Emerg. Infect. Dis.*, vol. 12, no. 11, pp. 1657-1662, Nov. 2006.

[5] Hinds W. C. 1999 Aerosol technology, 2nd edn. New York, NY: John Wiley and Sons, Inc.

[6] SETTLES, G. S. 2006 Fluid mechanics and homeland security. Annu. Rev. Fluid Mech. 38, 87–110.

[7] Ross, B. B., R. Gramiak, and H. Rahn. "Physical dynamics of the cough mechanism." *J Appl Physiol* 8, no. 3 (1955): 264-268.1955

[8] Chao CYH, Wan MP, Sze To GN, "Transport and removal of expiratory droplets in hospital ward environment," Aerosol Sci. Technol. 42, 377 – 394.

[9] Zhu S, Kato S, Yang J-H, "Study on transport characteristics of saliva droplets produced by coughing in a calm indoor environment," Build. Environ. 41, 1691– 1702. 2006

[10] Duguid JP, " The numbers and sites of origin of the droplets expelled during expiratory activities" Edinb. Med. J. 52, 385– 401. 1945

[11] Loudon RG, Roberts RM, "Droplet expulsion from respiratory tract" Am. Rev. Respir. Dis. 95, 435– 442. 1967

[12] Duguid JP, "The size and the duration of air-carriage of respiratory droplets and droplet-nuclei" J. Hyg. 44, 471– 479. 1946

[13] Gerone PJ, Couch RB, Keefer GV, Douglas RG, Derrenba EB, Knight V, "Assessment of experimental and natural viral aerosols." Bacteriol. 1966

[14] Xie X, Li Y, Sun H, Liu L. "Exhaled droplets due to talking and coughing," J. R. Soc. Interface 6, S703– S714. 2009

[15] Papineni RS, Rosenthal FS, "The size distribution of droplets in the exhaled breath of healthy human subjects," J. Aerosol Med. 10, 105– 116. 1997

[16] Chen, Z., and Zhao, B, "Some Questions on Dispersion of Human Ex- haled Droplets in Ventilation Room: Answers from Numerical Investigation. Indoor Air," 20:95–111. 2010

[17] Roy CJ, Milton DK, "Airbourne transimission of communicable infection -- the elusive pathway" N Engl J Med. 350: 1710-1712. 2004

[18] S. Fitzgerald, "ENGG460 Project Scope Document - Physiological Measurements of Human Coughs and Sneezes", Engineering principles and practice. 2016

46

[19] S. Fitzgerald, "ENGG460 Initial Literature Review - Physiological Measurements of Human Coughs and Sneezes", Engineering principles and practice. 2016

[20] S. Fitzgerald, "ENGG460 Draft Project Plan - Physiological Measurements of Human Coughs and Sneezes", Engineering principles and practice. 2016

[21] "K-epsilon models -- CFD-Wiki, the free CFD reference", *Cfd-online.com*, 2016. [Online]. Available: http://www.cfd-online.com/Wiki/K-epsilon_models.

[22] Prof. Franz Durst, "Turbulence Models and their applications", 10th indo German Winter Academy 2011
http://www.leb.eei.unierlangen.de/winterakademie/2011/report/content/course01/pdf/0112.pdf

[23] Meg VanSciver, Shelly Miler, Jean Hertzberg, "Particle Image Velocimetry of Human Cough", Department of Mechanical Engineering, University of Colorado. 45-415-422. 2011

[24] "HS RA 01 Working in an office environment | Health & Safety", *Safety.unsw.edu.au*, 2016. Available: http://safety.unsw.edu.au/hs-ra-01-working-office-environment.

[25] "pharynx | anatomy", *Encyclopedia Britannica*, 2016. Available: https://www.britannica.com/science/pharynx.

[26] Paul Stark, "Radiology of the trachea", Thieme Medical Publishers, Incorporated. 1991

[27] Renata de Cassia Gonçalves, Dirceu Barnabé Raveli, Ary dos Santos Pinto, "Effects of age and gender on upper airway, lower airway and upper lip growth", Department of Orthodontics, Faculdade de Odontologia de Araraquara, UNESP - Univ Estadual Paulista, Araraquara, SP, Brazil. 2011

[28] X.C.P van der Velden, "Numerical investigation of an upper airway in a patient suffering from stridor", Delft University of Technology. 2012

[29] "length and time scales in turbulent flows", Utah college of Engineering, 2016 Available: http://www.eng.utah.edu/~mcmurtry/Turbulence/turblt.pdf.

Consultation Meetings Attendance Form

Week	Date	Comments (if applicable)	Student's Signature	Supervisor's Signature
2	9/8/16	First Meeting Project Goals		
3	16/8/16	Learning Fluent		
4	23/8/16	Learning Fluent Turbulence Models		
5	30/8/16	Learning Fluent Turbulence Models		
6	6/9/16	Discuss Progress Report		
7	13/9/16	CFD on simple Geometry		
Mid-Sem	20/9/16	CFD Mesh size selection		
8	27/9/16	Create CAD model of upper airway		
9	4/10/16	CFD simulations on upper airway model		
10	11/10/16	Testing different turbulence models		

11	18/10/16	CFD of different upper airway shape		
12 13	25/10/16 1/11/16	Final Results Writing Thesis		